Current Research in Physiology 8 (2025) 100140

Contents lists available at ScienceDirect

Current Research in Physiology

journal homepage: www.sciencedirect.com/journal/current-research-in-physiology

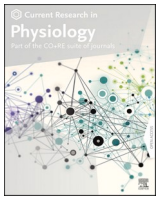

Microvascular endothelial cells display organ-specific responses to extracellular matrix stiffness

Rana Haidari [a,b,c], Wesley J. Fowler [d], Stephen D. Robinson [c,d], Robert T. Johnson [a,b,e,1,*], Derek T. Warren [a,b,**,1]

[a] School of Chemistry, Pharmacy and Pharmacology, University of East Anglia, Norwich Research Park, Norwich, NR4 7TJ, UK
[b] Biomedical Research Centre, University of East Anglia, Norwich Research Park, Norwich, NR4 7TJ, UK
[c] School of Biology, University of East Anglia, Norwich Research Park, Norwich, NR4 7TJ, UK
[d] Quadram Institute Bioscience, Norwich Research Park, NR4 7UQ, UK
[e] Department of Biomedicine, Aarhus University, 8000, Aarhus, Denmark

ARTICLE INFO

Keywords:
Ageing
Endothelial cell
Matrix stiffness
Mechanotransduction
Microvascular

ABSTRACT

The extracellular matrix was originally thought of as simply a cellular scaffold but is now considered a key regulator of cell function and phenotype from which cells can derive biochemical and mechanical stimuli. Age-associated changes in matrix composition drive increases in matrix stiffness. Enhanced matrix stiffness promotes the progression of numerous diseases including cardiovascular disease, musculoskeletal disease, fibrosis, and cancer. Macrovascular endothelial cells undergo endothelial dysfunction in response to enhanced matrix stiffness. However, endothelial cells are highly heterogeneous, adopting structural and gene expression profiles specific to their organ of origin. Endothelial cells isolated from different vessels (i.e. arteries, veins or capillaries) respond differently to changes in substrate stiffness. It is unknown whether microvascular endothelial cells isolated from different organs also display organ-specific responses to substrate stiffness. In this study, we compare the response of microvascular endothelial cells isolated from both the mouse lung and mammary gland to a range of physiologically relevant substrate stiffnesses. We find that endothelial origin influences microvascular endothelial cell response to substrate stiffness in terms of both proliferation and migration speed. In lung-derived endothelial cells, proliferation is bimodal, where both physiologically soft and stiff substrates drive enhanced proliferation. Conversely, in mammary gland-derived endothelial cells, proliferation increases as substrate stiffness increases. Substrate stiffness also promotes enhanced endothelial migration. Enhanced stiffness drove greater increases in migration speed in mammary gland-derived than lung-derived endothelial cells. However, stiffness-induced changes in microvascular endothelial cell morphology were consistent between both cell lines, with substrate stiffness driving an increase in endothelial volume. Our research demonstrates the importance of considering endothelial origin in experimental design, especially when investigating how age-associated changes in matrix stiffness drive endothelial dysfunction and disease progression.

1. Introduction

The endothelium, a single layer of squamous endothelial cells (ECs) that form a tube-like membrane, is ubiquitous throughout all vessels of the vasculature. Despite its ubiquity, the endothelium and the ECs that comprise it are highly heterogeneous, with endothelial structure and gene expression adopting organ-specific profiles (Gifre-Renom et al., 2022). Single-cell RNA-sequencing has identified that EC heterogeneity among different tissues is defined by the tissue itself, rather than the vessel types (i.e. arterial, capillary, venous) that permeate it (Kalucka et al., 2020). In mature vasculature, the endothelium exists in a quiescent state, with minimal EC proliferation and migration. However, endothelial quiescence is not a passive state, since biochemical and mechanical signalling inputs are required to maintain quiescence (Ricard et al., 2021).

This article is part of a special issue entitled: Physiology of Ageing published in Current Research in Physiology.

* Corresponding author. Department of Biomedicine, Aarhus University, 8000, Aarhus, Denmark.
** Corresponding author. School of Chemistry, Pharmacy and Pharmacology, University of East Anglia, Norwich Research Park, Norwich, NR4 7TJ, UK.
E-mail addresses: rob.johnson@biomed.au.dk (R.T. Johnson), derek.warren@uea.ac.uk (D.T. Warren).

[1] These authors contributed equally.

https://doi.org/10.1016/j.crphys.2025.100140
Received 23 July 2024; Received in revised form 21 October 2024; Accepted 24 January 2025
Available online 28 January 2025

Abbreviations

aEC	(aortic endothelial cell)
CVD	(cardiovascular disease)
EC	(endothelial cell)
ECM	(extracellular matrix)
FA	(focal adhesion)
LmEC	(lung-derived microvascular endothelial cell)
HUVEC	(human umbilical vein endothelial cell)
mEC	(microvascular endothelial cell)
MmEC	(mammary gland-derived microvascular endothelial cell)
PAH	(polyacrylamide hydrogel)
ROI	(Region of interest),
VEGF	(vascular endothelial growth factor)
VEGFR2	(VEGF receptor 2)

External mechanical cues, derived from either blood flow or the surrounding extracellular matrix (ECM), can either maintain endothelial quiescence or lead to EC activation (Dessalles et al., 2021). Mechanical stimuli are converted into biochemical signals either through activation of mechanosensitive membrane-embedded ion channels or through direct contact with the ECM at integrin-based focal adhesions (Alenghat and Ingber, 2002; Ohashi et al., 2017). Focal adhesions are sites of bidirectional communication. "Outside-in signalling" provides the cell with mechanical and biochemical signals from the ECM that regulate cytoskeletal structure, gene transcription, and cell survival (Miller et al., 2020). If transplanted onto a different ECM, cells can drastically change their phenotype (Statzer et al., 2023). Young ECMs can rescue cells from senescence, whilst old ECMs induce premature ageing (Statzer et al., 2023). Conversely, cells can reorganise their ECM through "inside-out signalling", whereby cellular forces can shape the ECM and in turn influence the cell's own phenotype (Gjorevski and Nelson, 2009).

Age-associated changes in ECM composition are well documented. For example, ECM stiffness increases with age (Schnellmann et al., 2022; Statzer et al., 2023). The correlation between ageing and ECM stiffness is so strong that changes to the mechanical properties of cells and tissues have been proposed as one of the new hallmarks of ageing (Schmauck-Medina et al., 2022). Ageing is the primary risk factor for numerous types of diseases, including cardiovascular disease, neurodegenerative disorders, musculoskeletal disorders, cancer, and fibrosis (J. Guo et al., 2022; Niccoli and Partridge, 2012; Schmauck-Medina et al., 2022). Enhanced ECM stiffness has been shown to drive the progression of these diseases (Burgess et al., 2016; Cox and Erler, 2011; Lampi et al., 2017; Lu et al., 2011; Theocharis et al., 2019). Furthermore, endothelial dysfunction plays an important part in the progression of these diseases, through either excessive vascular growth or regression, or changes in endothelial barrier function and signalling pathways (Hooglugt et al., 2022; Hsu et al., 2019; Huang et al., 2017; Zuchi et al., 2020).

Numerous studies have shown altered ECM stiffness to be a driver of endothelial dysfunction in diseases that primarily affect the larger vasculature, i.e. atherosclerosis and hypertension (Huveneers et al., 2015; Mohindra et al., 2021; Xu et al., 2023). However, less is known about how ECM stiffness regulates the microvasculature. Changes in substrate stiffness promote changes in macrovascular endothelial spreading (Califano and Reinhart-King, 2010; Mason et al., 2013; Stroka and Aranda-Espinoza, 2011), proliferation (Ding et al., 2017), migration (Bordeleau et al., 2017; Canver et al., 2016), and sprouting (Mason et al., 2013). Substrate stiffness can modulate key endothelial signalling pathways, including the VEGF-VEGFR2, nitric oxide, calcium, and notch signalling pathways (Derricks et al., 2015; Kohn et al., 2015; Kretschmer et al., 2023; LaValley et al., 2017). Likewise, macrovascular endothelial response to mechanical stimuli, including fluid shear stress, are modulated by substrate stiffness (Kohn et al., 2015). Altered substrate stiffness also regulates endothelial integrin expression and activation, cytoskeleton organisation, contractility and EC stiffness (Byfield et al., 2009; Kretschmer et al., 2023; Sack et al., 2016; Stroka and Aranda-Espinoza, 2011). These studies were performed in either HUVECs (human umbilical vein endothelial cells) or bovine aortic ECs (aECs), two well characterised and easily obtainable EC lines. However, due to differences in endothelial response that can arise based on EC tissue or vascular origin, responses observed in these cell lines may not fully recapitulate how microvascular ECs (mECs) respond to changes in substrate stiffness.

A direct comparison of aortic, veinous, and microvascular ECs revealed that the vessel of origin regulates EC response to substrate stiffness (Wood et al., 2011). For example, whilst aortic and mEC proliferation was increased by enhanced substrate stiffness, veinous EC proliferation was not (Wood et al., 2011). Furthermore, a comparison of HUVECs versus immortalised human mECs revealed that these cell lines activated different signalling pathways in response to substrate stiffness (Bastounis et al., 2019). However, it was EC type and not substrate stiffness that drove transcriptional changes in these cells (Bastounis et al., 2019). It is unknown whether the organ mECs originate from affects how mECs respond to substrate stiffness. Existing studies that use organ-specific mECs do so to answer disease-specific questions (Juin et al., 2013; Mammoto et al., 2013; Shen et al., 2018). In this study, we therefore investigate whether mECs isolated from two different organs display a differential response to substrate stiffness.

We compare how mECs isolated from either the mouse lung or mammary gland respond to changes in substrate stiffness. Both organs possess a rich microvascular network (Moccia et al., 2023; Wu and Birukov, 2019) and a similar physiological stiffness. Both microvascular networks also experience considerable mechanical stimuli. The lungs are the most vascularised organ in the body and possess a microvascular network that is highly sensitive to changes in stress, strain, and matrix stiffness (Fang et al., 2019; Wu and Birukov, 2019). Meanwhile, the mammary gland is a highly dynamic organ. Puberty, pregnancy and menopause, in addition to the menstrual cycle, all alter the microvascular structure of the mammary gland (Moccia et al., 2023). Mammary gland microvascular expansion or regression is accompanied by extensive ECM remodelling, where changes in ECM composition and structure result in altered mammary gland stiffness (Schedin and Keely, 2011). A material's stiffness is defined by its Young's modulus (measured in pascals, Pa). Depending on the vascular bed, healthy vasculature has a basement membrane stiffness in the range of 2–70 kPa (Wood et al., 2011). However, the microvasculature's perceived extracellular stiffness comes mainly from its surrounding tissue (Dessalles et al., 2021). We therefore cultured lung and mammary gland-derived mECs on different stiffnesses of fibronectin-coated polyacrylamide hydrogels to mimic the stiffness of healthy, aged or diseased tissue. Our results reveal that the organ mECs originate from regulates mEC response to substrate stiffness. Whilst lung and mammary gland-derived mEC morphology responded similarly to increasing substrate stiffness, how these cells proliferated and migrated was dependent on their organ of origin.

2. Materials and methods

2.1. Polyacrylamide hydrogel fabrication

Polyacrylamide hydrogels (PAH) were prepared as described previously (Johnson et al., 2024a; Minaisah et al., 2016). Glass coverslips were activated by (3-Aminopropyl)triethoxysilane (2 min), washed 3x with dH_2O, then fixed in 0.5% glutaraldehyde (40 min). After fixation, coverslips were washed and air dried overnight. Buffers of varying acrylamide:bis-acrylamide concentrations were prepared (Table 1). These compositions have previously been confirmed to fabricate PAHs of 2–72 kPa stiffness (Minaisah et al., 2016; Moeller et al., 2018; Porter et al., 2020). To fabricate PAHs, the appropriate volume of buffer was

Table 1
– Polyacrylamide hydrogel buffer consistency.

Stiffness (kPa)	Acrylamide (%)	Bis-acrylamide (%)
2	5.0	0.10
12	7.5	0.15
25	10.0	0.25
72	10.0	0.50

supplemented with 10% APS (1:100) and TEMED (1:1000), then placed on a standard microscopy slide and covered with an activated coverslip. Once set, PAHs were washed 3x with dH_2O, crosslinked with sulfo-SANPAH (1:3000) under UV illumination (365 nm, 5 min) and finally functionalised with fibronectin (Millipore, FC010) (10 μg/ml, 10 min at 37 °C).

PAH stiffnesses (Table 1) were chosen to be approximations of the *in vitro* stiffnesses of the: healthy lung (Guimarães et al., 2020; Luque et al., 2013; Pospelov et al., 2023), healthy mammary gland (Acerbi et al., 2015; Paszek et al., 2005; Ramião et al., 2016), aged lung (Melo et al., 2014), fibrotic or cancerous lung (T. Guo et al., 2022; Kwon et al., 2020; Southern et al., 2016), or cancerous mammary gland (Acerbi et al., 2015; Paszek et al., 2005; Ramião et al., 2016).

2.2. Endothelial cell isolation and culture

Mouse lung-derived microvascular ECs (LmECs) were isolated from C57BL/6 mice, aged 8–12 weeks, as previously described (Reynolds and Hodivala-Dilke, 2006). For the isolation of mammary microvascular ECs (MmECs), number 4 abdominal mammary glands from female C57BL/6 mice were extracted and the lymph node excised prior to being homogenised and digested as per Reynolds and Hodivala-Dilke (2006). Once isolated, EC lines were immortalised via polyoma-middle-T-antigen retroviral transfection (Ellison et al., 2015). Endothelial identity was confirmed through Western blot analysis of known endothelial markers, MmECs (Sup.Fig.1) or shown previously for LmECs (Alghamdi et al., 2020).

ECs were cultured in a 1:1 mixture of DMEM low glucose: Ham's F12 nutrient mixture (Invitrogen), supplemented with 0.1 mg/ml heparin and 10% FBS, and used between passages 4–16. These are passages in which we have previously confirmed our immortalised mEC lines retain both expression of endothelial markers and normal endothelial characteristics (Ellison et al., 2015). During standard culturing, mECs were grown on tissue culture grade plastic. For experimental studies, mECs were detached from their plastic substrate (0.25% trypsin:EDTA) prior to being seeded onto glass coverslips or PAHs at a density of 10,000 cells per well of a 24-well plate.

2.3. Western blot

Lysates were generated in high-SDS lysis buffer (3% SDS, 60 mM sucrose, 65 mM Tris-HCl pH 6.8). SDS-Page and western blotting was performed as previously described (Benwell et al., 2022). Nitrocellulose membranes were blocked in 5% skimmed-milk powder prepared in 0.1% Tween-20/PBS (PBST) for 1 h. Membranes were washed 3x in PBST, then incubated overnight at 4 °C in primary antibody (1:1000) overnight. CD31 (Cell Signalling Technology, 77699, RRID:AB_2722705); Endomucin (Santa Cruz, Sc-65495, RRID:AB_2100037); ERG (Abcam, Ab92513, RRID:AB_2630401); LYVE1 (Abcam, Ab14917, RRID:AB_301509); PROX1 (Abcam, Ab11941, RRID:AB_298722); VE-cadherin (Abcam, Ab205336, RRID:AB_2891001); VEGFR2 (Cell Signalling Technology, 2479, RRID:AB_2212507). Loading control Hsp70 was used at 1:2000 (Santa Cruz, Sc-7298, RRID:AB_627761). Secondary antibodies were subsequently added (1:5000) for 2 h in the dark, prior to ECL addition and chemiluminescence detection. Goat-anti-Mouse-HRP (Dako, P0447, RRID:AB_2617137); Goat-anti-Rabbit-HRP (Dako, P0448, RRID:AB_2617138).

2.4. Immunofluorescence and EC area/volume analysis

Cells were fixed in 4% paraformaldehyde for 10 min, permeabilised in 0.5% NP40 for 5 min, then blocked with 3% BSA/PBS for 1 h. Primary staining was performed overnight at 4 °C in 3% BSA/PBS. For area/volume analysis, cells were stained against lamin A/C (1:200) (Merck, SAB4200236, RRID:AB_10743057). For focal adhesion analysis, cells were stained against paxillin (1:100) (Abcam, Ab32084, RRID:AB_779033). Secondary staining was performed in the dark for 2 h in 3% BSA/PBS using the appropriate Alexa Fluor™ 488 antibody (1:400) (Thermo Fisher Scientific, A-11001, RRID:AB_2534069; Thermo Fisher Scientific, A-11008, RRID:AB_143165). F-actin was visualised using Rhodamine Phalloidin (1:400) (Thermo Fisher Scientific, R145). Mounting media ± DAPI was used to place samples onto microscopy slides prior to 20x images being captured using a Zeiss LSM980-Airyscan confocal microscope. Cell area and volume was measured as previously described (Ahmed et al., 2022; Johnson et al., 2024a), using FIJI, open-source software (Schindelin et al., 2012).

2.5. Random migration

ECs were cultured for 12 h at 37 °C, 5% CO_2 on a Zeiss Observer 7. Five 10x magnification phase-contrast images per well were captured every 10 min. Individual cells were manually tracked using the Manual Tracking Fiji plug-in (Schindelin et al., 2012). Migration speed, distance, and displacement were subsequently calculated using the Ibidi Chemotaxis and Migration Tool.

2.6. Proliferation

ECs were cultured in the presence of BrdU (Invitrogen, B23151) (10 μM) for 17 h, at 37 °C, 5% CO_2. Cells were washed twice in PBS prior to 4% paraformaldehyde fixation for 10 min. DNA hydrolysis was performed by incubation in 1M HCl for 30 min, prior to permeabilisation in 0.25% Triton/PBS for 30 min, and blocking in Dako™ Protein Block, Serum-Free (Agilent, X0909) for 10 min. Cells were stained against BrdU (1:200) (Abcam, Ab1893, RRID:AB_302659) overnight at 4 °C in PBS. Secondary staining was performed in the dark for 2 h using an appropriate Alexa Fluor™ antibody (Invitrogen, A21436, RRID:AB_2535857). Samples were mounted onto microscopy slides using a DAPI-containing mounting media prior to 10x images being captured. Each image captured a 1300 × 1030 μm region of interest (ROI), with the proportion of BrdU + nuclei compared to the total number of nuclei calculated in each ROI.

2.7. Statistical analysis

Statistical analysis was performed using GraphPad Prism 9.5.1. Results are presented as a superplot. A black bar indicates the mean of 3 independent experiments ±SEM. Large, coloured symbols represent the means of individual experiments. These are overlaid on grey dots, which show the full spread of data across all experiments. The mean number of cells or ROIs analysed per experiment are detailed in the corresponding figure legend. Where two conditions were compared, normality was confirmed using the Shapiro–Wilk test, prior to an unpaired Student's t-test to test for significant differences between the means of 3 independent experiments. Where multiple conditions were compared, a one-way ANOVA was performed on the means of 3 independent experiments, followed by Tukey's multiple comparison test. To test for differences between two cell lines, experimental means for each condition were normalised to that cell line's mean response on glass. A two-way ANOVA, followed by Sidak's multiple comparisons test was then performed to test for differences between the experimental means of each cell line. Differences between conditions were considered statistically significant when $p < 0.05$. Non-significant (ns) comparisons where $p > 0.05$ are not highlighted on graphs.

3. Results

3.1. Substrate stiffness induced lung-derived microvascular endothelial cell spreading

We set out to determine if mECs from different organs display an organ-specific response to substrate rigidity. Immortalised, lung-derived mECs (LmECs) were detached from plastic tissue culture flasks and seeded overnight onto fibronectin coated hydrogels of 2, 12, 25 and 72 kPa stiffness. These stiffnesses approximate those experienced in the *in vivo* LmEC microenvironment in health (2 and 12 kPa), aged/pathological (25 kPa) and pathological (72 kPa) conditions (Guimarães et al., 2020; J. Guo et al., 2022; Luque et al., 2013; Melo et al., 2014; Pospelov et al., 2023). Traditional *in vitro* experiments utilise tissue culture glass or plastic, materials whose stiffness is approximately a thousand times greater than the mEC microenvironment (Minaisah et al., 2016; Wood et al., 2011). LmECs were therefore also cultured on fibronectin coated glass-coverslips, enabling us to compare their response on traditional tissue culture substrates versus substrates of physiological stiffness.

Using confocal microscopy, we assayed how substrate rigidity regulated LmEC morphology, through measurements of cell and nuclear area, volume, and height. On soft hydrogels (2 and 12 kPa) LmECs attached but maintained a rounded morphology (Fig.1A). As hydrogel rigidity increased, LmECs began to spread and cell area and volume increased (Fig. 1A–C). LmEC area and volume doubled when cultured on glass, as compared to the most rigid hydrogels (72 kPa) (Sup.Fig. 2A–C). LmEC height was greatest when seeded on 2 kPa hydrogels. As substrate rigidity increased, cell height decreased as LmECs spread (Fig.1A,D).

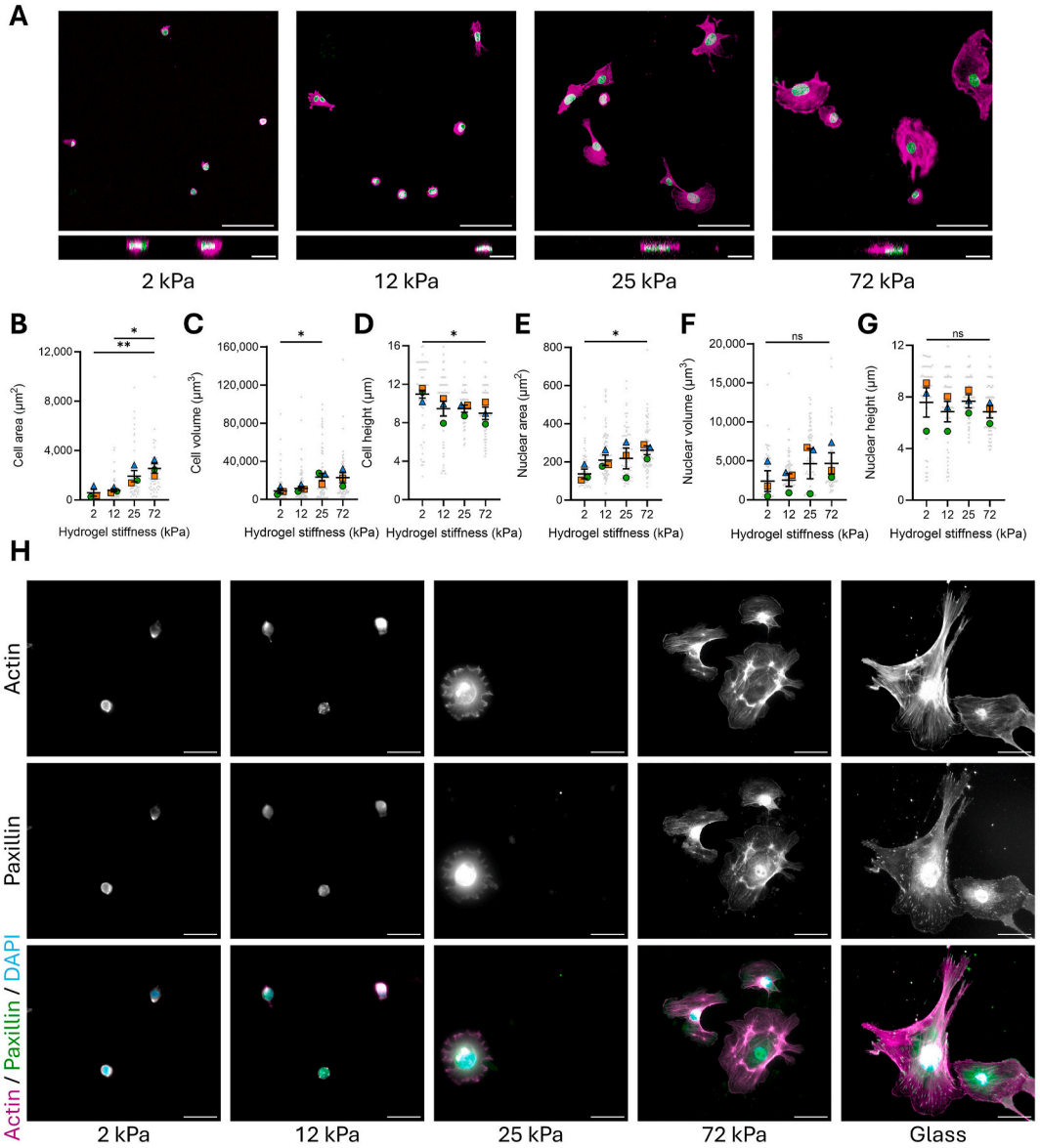

Fig. 1. Substrate stiffness induced lung-derived microvascular endothelial cell spreading. Lung-derived microvascular endothelial cells (LmECs) were seeded overnight onto fibronectin coated polyacrylamide hydrogels of varying stiffness (2, 12, 25 or 72 kPa). (A) Representative images of LmEC morphology. Actin cytoskeleton (purple) and lamin A/C labelled nuclei (green). Top – XY images of LmEC area. Scale bar = 100 μm. Bottom – XZ images of LmEC height. Scale bar = 20 μm. Analysis of LmEC Cell (B) area, (C) volume, (D) height, and nuclear (E) area, (F) volume, (G) height. (B–G) graphs are representative of 3 independent experiments, the means of which are shown as large, coloured symbols. An average of 24 cells per condition, per experiment were analysed. Small grey dots represent the measurement of 1 individual cell. Error bars = SEM. Significance determined using a one-way ANOVA with Tukey's post-hoc test. (ns = non-significant), (* = $p < 0.05$), (** = $p < 0.01$). (H) Representative images of LmEC actin cytoskeleton and paxillin labelled adhesions, seeded on hydrogels of varying stiffness (2, 12, 25 or 72 kPa) or glass-coverslips. Scale bar = 50 μm.

Despite further increases in LmEC area and volume, LmEC height was unchanged when cultured on glass-coverslips compared to 72 kPa hydrogels (Sup.Fig.2D). Substrate rigidity induced changes in nuclear area and volume were less clear but broadly followed the same trend as cell area and volume. As hydrogel rigidity increased, LmEC nuclear area and volume increased (Fig.1A,E & F). LmECs cultured on glass-coverslips compared to 72 kPa hydrogels displayed a further increase in nuclear area, but no reciprocal increase in nuclear volume (Sup. Fig.2E&F). LmEC nuclear height was unchanged across all substrate rigidities (Fig.1A,G & Sup.Fig.2G).

Having established substrate rigidity as a regulator of LmEC morphology, we next investigated in more detail how the actin cytoskeleton responded to changes in substrate stiffness. In response to internal or external stimuli, ECs are able to rapidly reorganise their actin cytoskeleton, thereby altering EC dynamics (Prasain and Stevens, 2009; Schnittler et al., 2014). In response to overnight seeding on soft substrates (2 kPa), cortical actin was observed at the cell periphery (Fig. 1H). As substrate stiffness increased (25 kPa), LmECs began to form actin-based protrusions (Fig. 1H). As stiffness increased further (72 kPa), actin stress fibres formed, with more prominent stress fibres observed in LmECs adhered to glass (Fig. 1H). Actin filaments respond to mechanical and biochemical signals from the ECM via their interaction with cell-substrate contact sites known as focal adhesions (FAs) (Ohashi et al., 2017). FAs are dynamic multiprotein structures that undergo rapid turnover in response to mechanical cues (Mishra and Manavathi, 2021). We therefore used paxillin as a FA marker to investigate how substrate stiffness regulated FA localisation in LmECs (Fig. 1H). LmECs adhered to glass displayed mature FA complexes that localised to the ends of actin stress fibres (Fig. 1H). In contrast, on soft substrates, distinguishable paxillin-positive FAs were not observed. Instead on 2 kPa substrates, and to a lesser extent 12 kPa substrates, paxillin co-localised with cortical actin. As LmECs spread, clusters of paxillin-positive nascent FAs were observed at the leading edges of lamellipodia along with nuclear accumulation of paxillin (25 kPa) (Fig. 1H). On the most rigid hydrogels (72 kPa), LmECs formed fibrillar adhesions (Fig. 1H).

3.2. Lung-derived microvascular endothelial cell proliferation and migration are regulated by substrate stiffness

Microvascular networks are quiescent, meaning that *in vivo* mECs typically undergo minimal or no proliferation or migration (Ricard et al., 2021). Isolation and *in vitro* culturing of ECs forces them into an artificially activated state where these processes and their regulation can be studied (Boisen et al., 2010). To determine the effect of substrate rigidity on mEC proliferation, we performed a BrdU assay, whereby LmECs were cultured overnight on hydrogels or glass-coverslips in the presence of BrdU. Nuclear incorporation of BrdU was assessed using immunofluorescence, and the proportion of BrdU + cells in each region was calculated. Analysis revealed that LmEC proliferation followed a bimodal distribution (Fig. 2A&B). Proliferation was highest when cells were seeded on the softest hydrogels (2 kPa) and lowest on 12 kPa hydrogels. On more rigid hydrogels, LmEC proliferation was still reduced compared to that observed on 2 kPa hydrogels. However, in comparison to LmECs seeded on 12 kPa hydrogels, LmECs on 25 and 72 kPa hydrogels trended to undergo a greater rate of proliferation, but this increase was not statistically significant (Fig. 2A&B). LmEC proliferation was unchanged on glass-coverslips (Sup.Fig.2H,I).

Having established that substrate rigidity regulated LmEC proliferation, we next used time-lapse microscopy to track LmEC migration on substrates of different stiffness over a 12-h period (Fig. 2C–F). LmEC migration speed and migration distance was greatest on the stiffest substrates (72 kPa hydrogels and glass) (Fig.2D,E & Sup.Fig. 2J–L). On softer substrates ($\leq$25 kPa), LmEC migration was reduced (Fig. 2C–E). However, when we calculated LmEC displacement (a straight-line measurement between the first and last positions the cell was observed at), we see that increased substrate stiffness drove an increase in LmEC displacement (Fig. 2F). Displacement provides us with a measurement of how persistent or directional a cell's migration is. Low displacement indicates that even though a cell may be moving, overall, it is merely moving around a point without travelling anywhere. Conversely, high displacement indicates that a cell has persistently migrated away from a point in one main direction. Analysis of our data indicated that LmEC migration is more random on the softest substrate (2 kPa). LmEC displacement increased as substrate stiffness increased, therefore LmEC migration was the most directional on the stiffest hydrogels (72 kPa) (Fig. 2F). LmEC displacement was unchanged in cells on 72 kPa hydrogels versus glass-coverslips (Sup.Fig.2M).

3.3. Substrate stiffness induced mammary gland-derived microvascular endothelial cell spreading

Having established that substrate rigidity regulated LmEC morphology, proliferation and migration, we next sought to determine if these effects differed in mECs isolated from a different organ. We therefore repeated the above experiments, this time using mammary gland-derived mECs (MmECs). The lung and mammary gland are both microvascular rich organs (Moccia et al., 2023; Wu and Birukov, 2019), but most studies suggest that the mammary gland is a softer organ than the lung (Acerbi et al., 2015; Guimarães et al., 2020; Luque et al., 2013; Paszek et al., 2005; Pospelov et al., 2023; Ramião et al., 2016). We therefore hypothesised that the responses to substrate stiffness we observed in LmECs may occur earlier in MmECs, with changes being driven by the relative increase in substrate stiffness, not purely the physical stiffness.

MmECs were cultured overnight on fibronectin-coated hydrogels of increasing rigidity or glass-coverslips. Confocal microscopy revealed that substrate rigidity induced similar changes in MmEC morphology to those observed in LmECs (Fig. 3A, Sup.Fig. 3A–G). On the softest substrates, MmECs were rounded and increased substrate stiffness once again drove cell spreading (Fig. 3A,B). MmEC volume also increased as hydrogel stiffness increased, with MmEC area and volume greatest when cells were cultured on glass-coverslips (Fig. 3A–C, Sup.Fig. 3A–C). Cell and nuclear height were greatest on the 2 kPa hydrogels. Cell height reduced as cells became less rounded on 25 kPa hydrogels. As substrate stiffness increased further, no additional reduction in cell height was observed (Fig. 3A,D, & Sup.Fig.3A,D). Nuclear height followed the same trend, but also underwent an additional reduction when MmECs were cultured on glass (Fig. 3A,G & Sup.Fig.3A,G). MmEC nuclear area and volume enlarged as substrate stiffness increased (Fig. 3A,E & F). As observed in LmECs, MmECs cultured on glass-coverslips compared to 72 kPa hydrogels displayed an increase in nuclear area but no corresponding increase in nuclear volume (Sup.Fig.3A,E & F).

A closer look at MmEC actin filament organisation revealed a similar response to enhanced substrate stiffness as that observed in LmECs. On the softest substrate (2 kPa), cortical localisation of actin is observed (Fig. 3H). As cells spread, actin-based protrusions are observed (12 kPa) and become more prominent on 25 kPa hydrogels. Further increases in substrate stiffness resulted in stress fibre formation (72 kPa), with the most prominent stress fibres observed in MmECs cultured on glass (Fig. 3H). Paxillin localisation also followed similar trends. On glass, paxillin localised to mature FAs whilst on 72 kPa hydrogels paxillin-positive fibrillar adhesions were observed (Fig. 3H). On softer substrates, paxillin-positive nascent adhesions were found at the leading edge of lamellipodia (25 kPa and some 12 kPa cells). In these cells, paxillin also localised to the nucleus. Finally, on 2 kPa hydrogels, paxillin localised with cortical actin (Fig. 3H).

3.4. Mammary gland-derived microvascular endothelial cell proliferation and migration is driven by enhanced substrate stiffness

We next assayed whether enhanced substrate stiffness also drove changes in MmEC proliferation and migration. Immunofluorescent

analysis of BrdU incorporation revealed that substrate stiffness induced a different proliferation response in MmECs compared to LmECs. We found that MmEC proliferation was lowest on the softest hydrogels (2 kPa) (Fig. 4A and B). On substrates stiffer than 2 kPa, MmEC proliferation was increased (Fig. 4A and B & Sup.Fig. 3H and I). Enhanced substrate stiffness also promoted MmEC migration (Fig. 4C–F). However, we observed subtle differences between the migration of MmECs and LmECs over the range of substrate rigidities assayed. MmECs migrated faster and more directly when hydrogel rigidity was 25 kPa or greater (Fig. 4C–F). Meanwhile in LmECs, this response was only observed when substrate rigidity was 72 kPa or greater (Fig. 2C–F). Furthermore, when we compared MmEC migration on glass versus our stiffest pathologically relevant substrate (72 kPa), MmEC migration speed and distance were found to be greater on the 72 kPa substrate than on glass (Sup.Fig. 3J–M).

3.5. Microvascular endothelial cell response to substrate stiffness is regulated by endothelial origin

Finally, we sought to confirm if LmECs and MmECs underwent a differential response to substrate stiffness. Therefore, we normalised the experimental means obtained at each stiffness to that cell line's mean response on glass. This normalisation was performed to account for any inherent differences between the two cell lines, thereby enabling only substrate stiffness dependent responses to be compared. mEC response on glass was chosen as our comparative reference for two reasons. Firstly, traditional experiments are performed on glass or plastic substrates. Secondly, for most parameters assayed, mEC response was greatest when cultured on glass. Comparison of mEC morphology revealed that whilst substrate stiffness promoted mEC spreading, this response was comparable in both LmECs and MmECs, with no differences in cell or nuclear area, volume or height (Fig. 5A–F). Comparing proliferation and migration between the two lines revealed that mEC origin influenced the cells' response to substrate stiffness. LmEC and MmEC proliferation was significantly different on the softest substrates

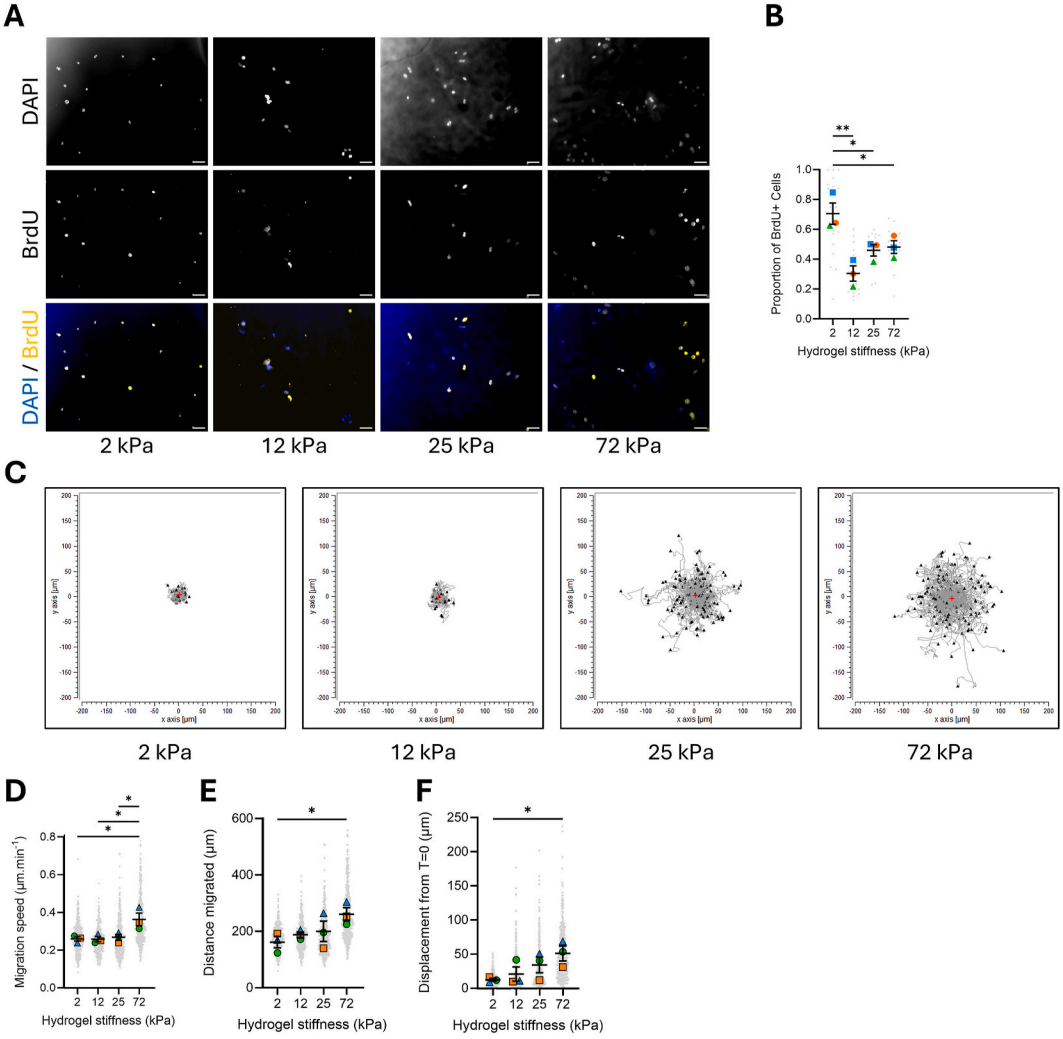

Fig. 2. Lung-derived microvascular endothelial cell proliferation and migration are regulated by substrate stiffness. Lung-derived microvascular endothelial cells (LmECs) seeded on fibronectin coated polyacrylamide hydrogels of varying stiffness (2, 12, 25 or 72 kPa). (A) Representative immunofluorescence images of BrdU incorporation and DAPI nuclear stain. Scale bar = 100 µm. (B) LmEC proliferation. Representative of 3 independent experiments, the means of which are shown as large, coloured symbols. An average of 6 ROIs per condition, per experiment were analysed. Small grey dots represent the analysis of 1 individual ROI. Analysis of LmEC migration (C) representative migration tracks (all tracks forced to originate at coordinate 0,0), graphs of (D) speed, (E) distance, and (F) displacement. Representative of 3 independent experiments, the means of which are shown as large, coloured symbols. An average of 113 cells per condition, per experiment were analysed. Small grey dots represent the measurement of 1 individual cell. (D-F) Error bars = SEM. Significance determined using a one-way ANOVA with Tukey's post-hoc test. (* = $p < 0.05$), (** = $p < 0.01$).

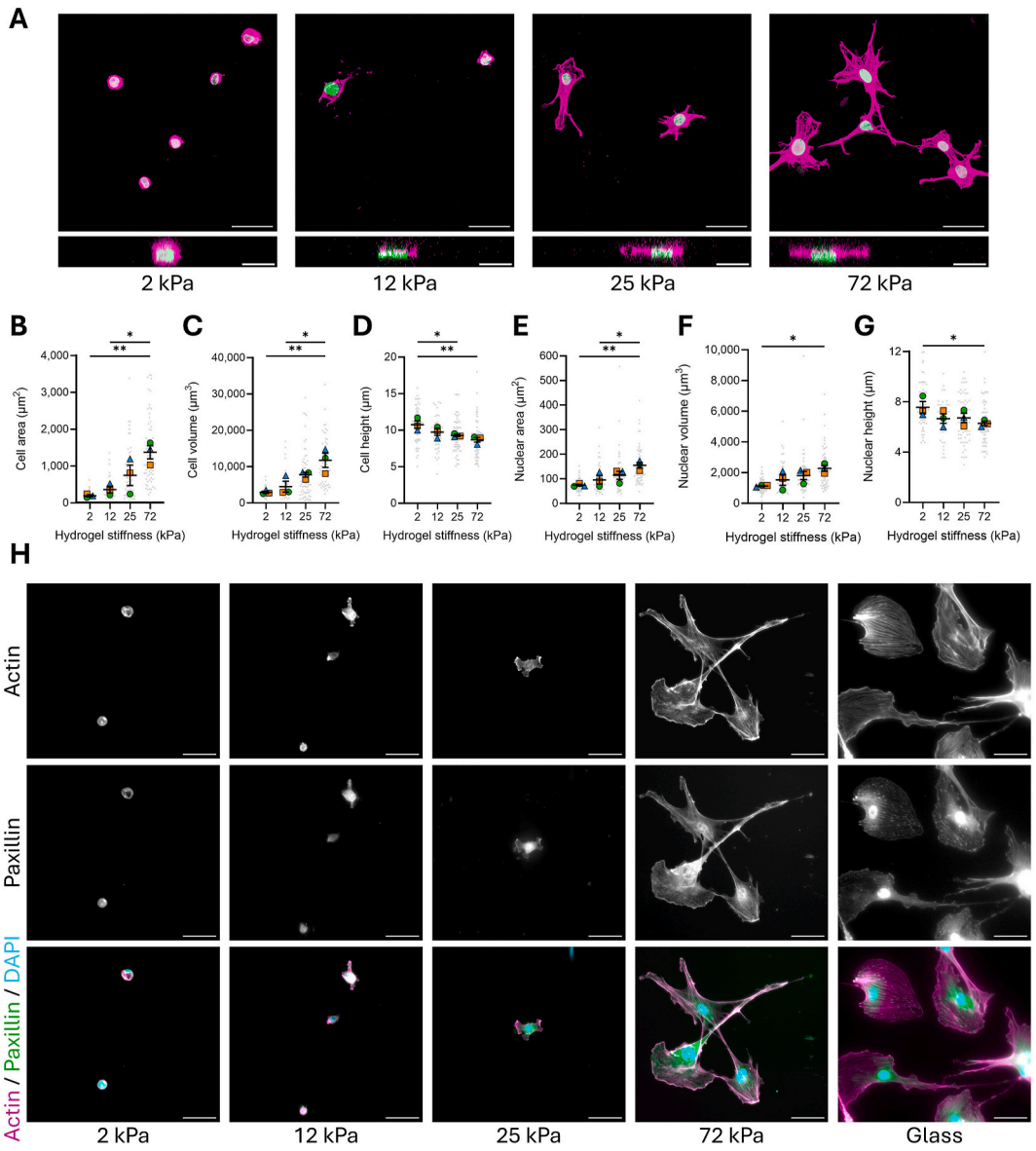

Fig. 3. Substrate stiffness induced mammary gland-derived microvascular endothelial cell spreading. Mammary gland-derived microvascular endothelial cells (MmECs) were seeded overnight onto fibronectin coated polyacrylamide hydrogels of varying stiffness (2, 12, 25 or 72 kPa). (A) Representative images of MmEC morphology. Actin cytoskeleton (purple) and lamin A/C labelled nuclei (green). Top – XY images of MmEC area. Scale bar = 50 μm. Bottom – XZ images of MmEC height. Scale bar = 20 μm. Analysis of MmEC Cell (B) area, (C) volume, (D) height, and nuclear (E) area, (F) volume, (G) height. (B–G) graphs are representative of 3 independent experiments, the means of which are shown as large, coloured symbols. An average of 23 cells per condition, per experiment were analysed. Small grey dots represent the measurement of 1 individual cell. Error bars = SEM. Significance determined using a one-way ANOVA with Tukey's post-hoc test. (* = $p < 0.05$), (** = $p < 0.01$). (H) Representative images of MmEC actin cytoskeleton and paxillin labelled adhesions, seeded on hydrogels of varying stiffness (2, 12, 25 or 72 kPa) or glass-coverslips. Scale bar = 50 μm.

(2 and 12 kPa hydrogels) (Fig. 5G). Over this stiffness range, these cells displayed opposing responses, with LmECs becoming less proliferative and MmECs more proliferative as stiffness increased from 2 to 12 kPa (Fig. 5G). Regarding migration, both mEC lines migrated faster and further as substrate stiffness increased (Fig. 5H–J). However, substrate stiffness had a more pronounced effect on MmECs compared to LmECs. Specifically, when cultured on 25 or 72 kPa hydrogels, MmECs displayed a significantly higher relative migration speed than LmECs (Fig. 5H).

4. Discussion

In the present study, we show that mEC response to substrate stiffness is regulated by their organ of origin (Fig. 6). This builds on previous studies that found that ECs from arteries, veins or the microvasculature produce differential responses to changes in substrate stiffness (Wood et al., 2011). Specifically, we demonstrate that substrate stiffness induces a differential response in mEC proliferation and migration, depending on the organ mECs were derived from. However, not all mEC responses were different. Substrate stiffness-induced changes in mEC morphology were consistent between the two cell lines assayed. Our research demonstrates the importance of considering endothelial origin when investigating how age-associated changes in matrix stiffness drive endothelial dysfunction and disease progression.

In discussing our findings, we consider the following necessary limitations to our study. Firstly, we used a single cell, two-dimensional approach. This is different from how the endothelium is organised *in vitro*, but it enabled us to easily measure endothelial response to

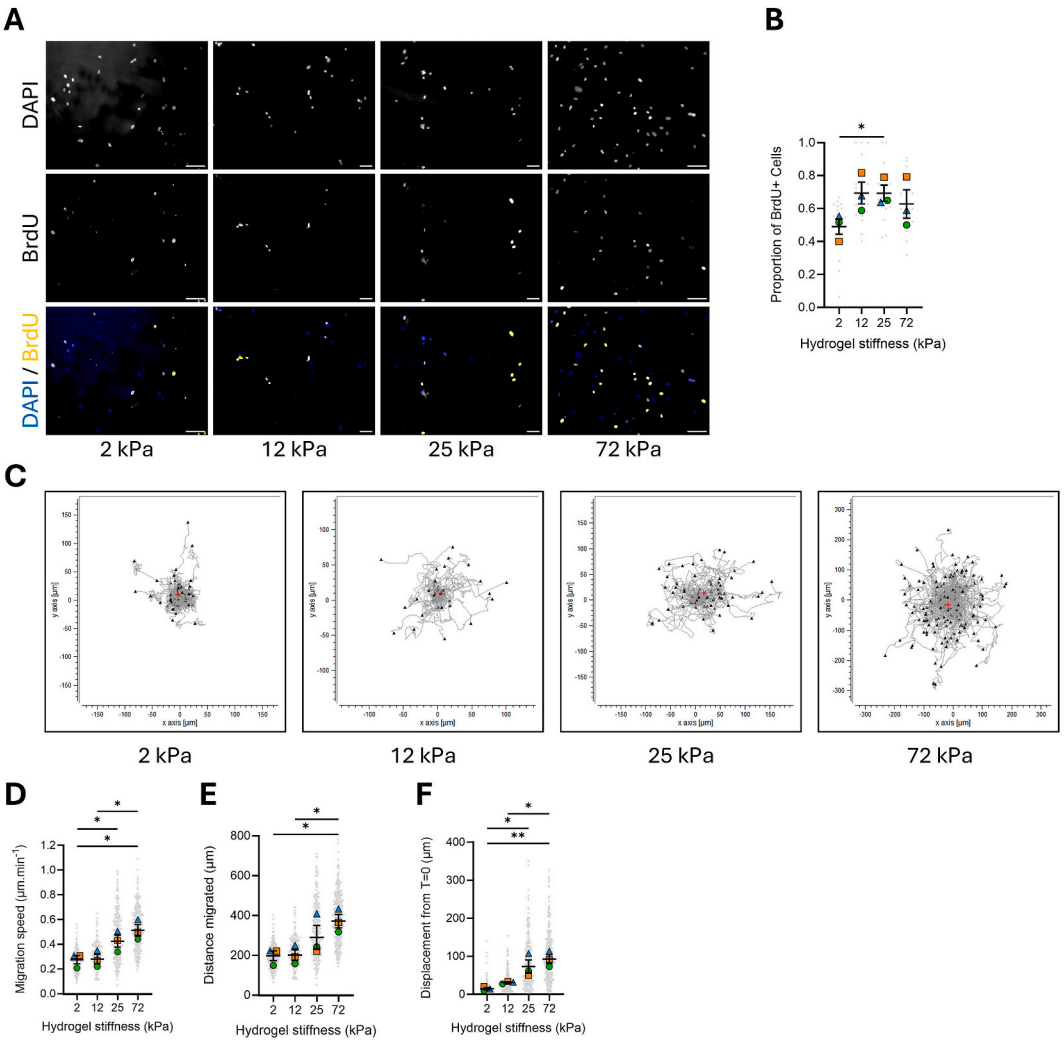

Fig. 4. Mammary gland-derived microvascular endothelial cell proliferation and migration is driven by enhanced substrate stiffness. Mammary gland-derived microvascular endothelial cells (MmECs) seeded on fibronectin coated polyacrylamide hydrogels of varying stiffness (2, 12, 25 or 72 kPa). (A) Representative immunofluorescence images of BrdU incorporation and DAPI nuclear stain. Scale bar = 100 µm. (B) MmEC proliferation. Representative of 3 independent experiments, the means of which are shown as large, coloured symbols. An average of 6 ROIs per condition, per experiment were analysed. Small grey dots represent the analysis of 1 individual ROI. Analysis of MmEC migration (C) representative migration tracks (all tracks forced to originate at coordinate 0,0), graphs of (D) speed, (E) distance, and (F) displacement. Representative of 3 independent experiments, the means of which are shown as large, coloured symbols. An average of 111 cells per condition, per experiment were analysed. Small grey dots represent the measurement of 1 individual cell. (D-F) Error bars = SEM. Significance determined using a one-way ANOVA with Tukey's post-hoc test. (* = $p < 0.05$), (** = $p < 0.01$).

substrate stiffness. Secondly, we used immortalised mECs. Immortalised mECs are a good *in vitro* model of EC behaviour that can provide the numbers of cells required to perform preliminary biochemical assays without excessive animal usage (Atkinson et al., 2018; Benwell et al., 2024; Ni et al., 2014; Tavora et al., 2014). Whilst primary ECs potentially respond differently to some stimuli, primary ECs are also not fully representative of *in vivo* mECs, as isolation and culturing places mECs into an artificially active state (Boisen et al., 2010). Finally, we only considered the impact of substrate stiffness. However, during ageing, blood pressure and fluid shear stress are also altered, with changes in substrate stiffness shown to modulate endothelial response to fluid shear stress (Kohn et al., 2015). Despite these limitations, our findings highlight the role that endothelial origin can play in regulating mEC response to substrate stiffness. Further research is now required to delineate the molecular mechanisms through which age-associated changes in matrix stiffness drive endothelial dysfunction in an organ-specific manner.

4.1. Published studies display considerable variation in their measurements of tissue stiffness

We assayed LmEC and MmEC response over a stiffness range that mimicked the *in vivo* stiffnesses of these organs in healthy (2 and 12 kPa), aged/pathological (25 kPa) and pathological (72 kPa) states. Knowledge of lung and mammary gland stiffness were obtained from published sources, with most studies suggesting that the healthy mammary gland (0.2–3 kPa) is slightly softer than the healthy lung (1–20 kPa) (Acerbi et al., 2015; Guimarães et al., 2020; Luque et al., 2013; Paszek et al., 2005; Pospelov et al., 2023; Ramião et al., 2016). However, some studies disagree with this statement and find the mammary gland to be the stiffer organ (Butcher et al., 2009; Chanda and Singh, 2023). Overall, there is considerable discrepancy in the published properties of biological tissues. One review found that the reported stiffness of the same tissue can vary by several orders of magnitude (McKee et al., 2011). Sample preparation and the techniques used to measure it can affect the readout of a tissue's mechanical properties (Guimarães et al., 2020; Navindaran et al., 2023). For example, decellularised or

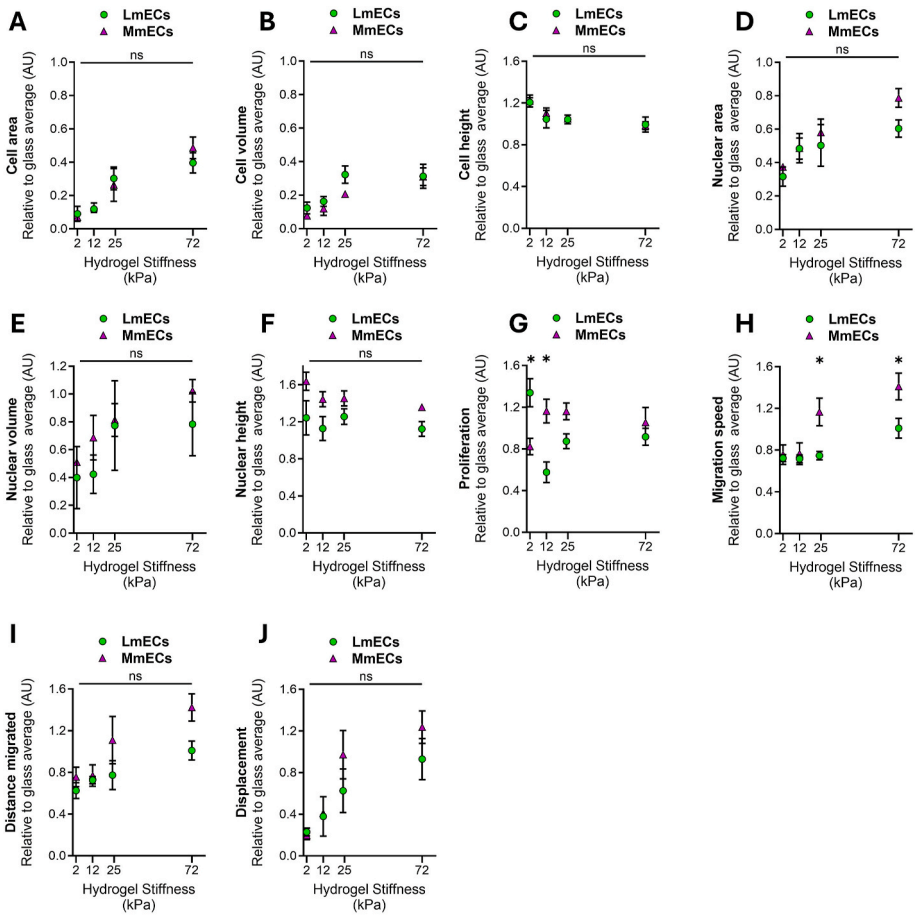

Fig. 5. Microvascular endothelial cell response to substrate stiffness is regulated by endothelial origin. For each microvascular endothelial cell (mEC) line, experimental means for each stiffness were normalised to their mean response on glass, enabling a direct comparison between lung (LmEC) and mammary gland (MmEC) derived mECs to be made. Graphs show a comparison of LmEC vs MmEC response to substrate stiffness. Morphology: Cell (A) area, (B) volume, (C) height. Nuclear (D) area, (E) volume, and (F) height. (G) Proliferation. Migration: (H) speed, (I) distance, and (J) displacement. Data representative of 3 independent experiments. Error bars = SEM. Significance determined using a two-way ANOVA with Sidak's multiple comparisons test. (*ns* = non-significant), (* = $p < 0.05$).

dehydrated tissues are typically stiffer than those in their native state (Guimarães et al., 2020). These factors make it difficult to compare the stiffness of two tissues, or the same tissue in different physiological states. Even when comparing the same tissue, with the same technique, the inherent variability of the results obtained can make it hard to derive a definitive readout of a tissue's mechanical properties between two different studies (Guimarães et al., 2020). In this study, we show that mEC origin can influence endothelial response to substrate stiffness. However, without reliable knowledge of how a tissue's stiffness changes over time or during disease progression, we cannot be confident of the translatability of our findings. Whilst tissue stiffness in general is known to increase with age, very few studies have physically measured how the stiffness of specific tissues changes during development and ageing (Schnellmann et al., 2022; Statzer et al., 2023). To enable future studies to better understand how matrix stiffness regulates the behaviour of endothelial and other cell types in an organ-specific manner, we propose that longitudinal studies of tissue stiffness are required. Importantly, these studies should simultaneously compare the stiffness of multiple tissues across the same developmental and adult timepoints. This would aid our understanding of the relative changes in tissue stiffness, both within the same organ and between different organs, that occur during development and ageing.

Furthermore, the potential of sex-based differences in tissue stiffness, and how that stiffness changes over time, should not be forgotten. In aged individuals, sex-specific differences in brain and skeletal muscle stiffness are known to exist (Arani et al., 2015; Eby et al., 2015). However, in the studies used to obtain our lung and mammary gland stiffnesses, only one specified that their measurements of tissue stiffness were performed on organs extracted from female mice (Pospelov et al., 2023). Whilst measurements of mammary gland stiffness can largely be presumed to be taken from females, the same cannot be presumed with measurements of lung stiffness. Biological sex has long been viewed as a risk factor for cardiovascular disease (CVD), with the incidence of CVD typically higher in men. However, CVD morbidity is greater in woman, partially due delays in diagnosis and treatment of this disease (Connelly et al., 2021; Gao et al., 2019; Gauci et al., 2022). In cardiac ageing, left ventricular thickness can be used to predict the incidence of adverse cardiac events (Merz and Cheng, 2016). However, ventricular thickness across all ages is greater in men than woman, but during CVD women experience a greater acceleration of ventricular thickening (Merz and Cheng, 2016). Differences based on biological sex have also been found at a cellular level. Gene expression in ECs differs between the sexes from birth, with further transcriptional differences accrued over time following exposure to sex hormones (Hartman et al., 2020). These findings highlight that biological sex is an important variable to consider when studying the mechanisms of ageing.

4.2. *Microvascular endothelial cell origin regulates stiffness-dependent changes in endothelial proliferation*

Physiologically relevant increases in matrix stiffness promote increased proliferation within HUVEC and bovine pulmonary aECs

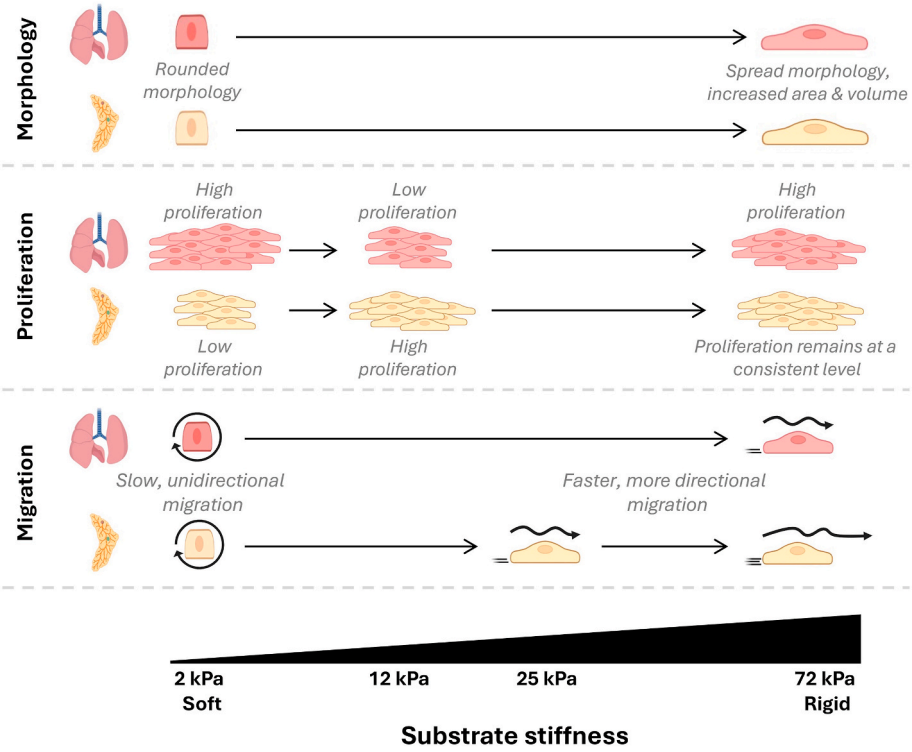

Fig. 6. Microvascular endothelial cells display organ-specific responses to extracellular matrix stiffness. Illustrative summary. Microvascular endothelial cells from mouse lung (LmEC) and mammary gland (MmEC) were cultured on polyacrylamide hydrogels that mimicked physiological and pathological matrix stiffness. Both cell types exhibited increased cell spreading, area, and volume as substrate stiffness increased. Meanwhile, proliferation and migration responses were dependent on the endothelial organ of origin. MmEC proliferation increased with substrate stiffness, whilst LmECs displayed a biomodal response (high on soft and rigid substrates, low on physiological stiffnesses). Both cell types migrated faster and more persistently as substrate stiffness increased. However, this response was observed in MmECs on softer substrates compared to LmECs.

(Ding et al., 2017; LaValley et al., 2017). However, this response plateaus in HUVECs on substrates stiffer than 21.5 kPa, whereby HUVEC proliferation remains constant despite further increases in substrate stiffness (Yeh et al., 2012). Conversely, cardiac mEC proliferation is unaffected by substrate stiffness increasing from 14 to 34 kPa (Shen et al., 2018). In our study, enhanced substrate stiffness drove increased proliferation in both lung (12–25 kPa) and mammary gland (2–12 kPa) derived mECs. As observed in HUVECs, further increases in matrix stiffness yielded no further increase in LmEC or MmEC proliferation, even when cultured on glass. Unlike MmECs, LmEC proliferation did not follow an exponential plateau relationship with substrate stiffness. Instead, LmEC proliferation appeared bimodal, with the greatest LmEC proliferation observed on the softest substrate (2 kPa). This observation might be explained through a developmental perspective. During development, tissues start soft and stiffen over time, with increases in stiffness typically coinciding with cellular differentiation (Guimarães et al., 2020; T. Guo et al., 2022). Based on our findings, we hypothesise that on 2 kPa substrates, LmECs revert to a developmental, proliferative phenotype. Previous studies have shown that human LmECs are sensitive to both enhanced and reduced substrate stiffness, whereby deviation from normal lung stiffness triggers reduced endothelial junctional integrity and vascular leakage (Mammoto et al., 2013). In our study, MmEC proliferation plateaued on substrates $\geq$12 kPa, whilst LmEC proliferation plateaued on substrates $\geq$25 kPa. This suggests that MmEC proliferation is sensitive to a lower range of substrate stiffnesses than LmECs. These differences may be explained by the *in vivo* stiffness of the mammary gland, which on average is found to be softer than the lung (Section 4.1). If softer substrates are reminiscent of an organ's endothelial microenvironment during development, we hypothesise that when MmECs are cultured on substrates softer than 2 kPa, they would also enter a hyperproliferative state, similar to that observed in LmECs on 2 kPa substrates. For this hypothesis to be tested, we first need to measure how the stiffness of the mammary gland changes during developmental processes, such as puberty.

4.3. *Microvascular endothelial cell origin regulates stiffness-induced changes in endothelial migration*

Increased substrate stiffness is known to promote both cardiac mEC random migration and porcine aEC collective migration (Canver et al., 2016; Shen et al., 2018). Furthermore, when presented with a stiffness gradient, HUVECs undergo durotaxis and preferentially migrate towards areas of greater stiffness (Zhong et al., 2020). However, in 3D cultures, bovine aEC migration is reduced by increased substrate stiffness (Bordeleau et al., 2017; Mason et al., 2013). We found that enhanced substrate stiffness increased endothelial migration speed, distance migrated and displacement in both LmECs and MmECs. Incremental changes in substrate stiffness led to increased MmEC migration, whilst in LmECs, migration speed only increased when cells were cultured on 72 kPa substrates. Furthermore, MmEC migration was greatest on the stiffest physiologically relevant substrate assayed (72 kPa) and subsequently decreased when MmECs were cultured on glass. However, LmEC migration was unchanged between these two substrates. The mammary gland is one of the few organs that undergo angiogenesis during adult life (Moccia et al., 2023). Physiological processes, including the menstrual cycle, puberty and pregnancy, promote regular remodelling of the mammary gland ECM, changing its composition and stiffness (Schedin and Keely, 2011). Based on our findings, we propose that the cyclic nature of the mammary gland programmes MmECs to be responsive to incremental changes in substrate stiffness. Meanwhile, in the healthy lung, quiescence maintains ECM composition. Stiffness-induced activation of LmECs is not required for physiological function, therefore LmEC

migration is not promoted by small increases in substrate stiffness. Our findings add to previous observations that show cell behaviour can be programmed by ECM stiffness. For example, following mechanical priming, lung fibroblasts maintain a fibrotic phenotype when transplanted from stiff to soft substrates (Balestrini et al., 2012). Meanwhile, transplantation from soft to stiff partially prevents the onset of a fibrotic phenotype (Balestrini et al., 2012).

4.4. Increased substrate stiffness drives increased microvascular endothelial cell volume in both lung and mammary gland-derived microvascular endothelial cells

Stiffness induced changes in endothelial morphology occur independently of endothelial origin. Increased substrate stiffness promoted endothelial spreading in both LmECs and MmECs, recapitulating observations made in bovine aECs and HUVECs (Califano and Reinhart-King, 2010; Mason et al., 2013). In both LmECs and MmECs, enhanced substrate stiffness induced an increase in EC volume. Increased cell volume is part of a hypertrophic response, whereby overall tissue volume increases without a corresponding increase in cell number. Endothelial hypertrophy results in reduced vascular perfusion and is a precursor to diseases including cardiac hypertrophy and ischemic retinopathies (Hofman et al., 2001; Jacques and Bkaily, 2019). Furthermore, anti-VEGF therapy induces glomerular EC hypertrophy and detachment, contributing to the onset of kidney disease in mice (Sugimoto et al., 2003). Our data suggests that endothelial hypertrophy may also be induced by enhanced matrix stiffness. We recently reported that a similar response is observed in vascular smooth muscle cells (Johnson et al., 2024a; Johnson et al., 2024b). Since matrix stiffness increases with age, stiffness-induced endothelial hypertrophy may therefore be a key driver of age-associated vascular dysfunction. However, this is only a preliminary finding. Further research is needed to firstly confirm that increased substrate stiffness induces a hypertrophic response within mECs, and secondly to delineate the molecular mechanisms responsible for this response.

Finally, we demonstrate that mEC actin cytoskeleton and FA organisation is regulated by substrate stiffness. This is in line with previous research that shows enhanced substrate stiffness increases actin expression and stress fibre formation in bovine aECs (Byfield et al., 2009). We now show that in both LmECs and MmECs, enhanced substrate stiffness promotes actin cytoskeleton remodelling, transitioning from cortical structures to dense actin stress fibres. Formation of actin stress fibres enables mECs to generate actomyosin-derived contractile forces that are capable of remodelling the ECM (Lee and Kumar, 2016). However, excessive contractility or force generation reduces endothelial barrier integrity and drives angiogenesis (Schnellmann et al., 2022). Whilst we demonstrate that substrate stiffness promotes the development of an actin-network, the network observed when mECs are cultured on glass is far more mature than that found when mECs were grown on our stiffest (72 kPa) pathologically relevant substrate. In vascular smooth muscle cells it is known that mechanical loading promotes the reorganisation and maturation of the actin cytoskeleton (Johnson et al., 2021). Glass is approximately a thousand times stiffer than the endothelial microenvironment, as such mECs cultured on glass are exposed to a greater mechanical load (Minaisah et al., 2016; Wood et al., 2011). *In vivo,* matrix stiffness is one of many forces that act on ECs (Dessalles et al., 2021). We therefore hypothesise that mature actin-networks, like the one we observed when mECs were cultured on glass can develop *in vivo* through the summation of multiple mechanical inputs. One potential force that may aid in the development of mature actin-networks is fluid shear stress.

Shear stress is the tangential force experienced by the endothelium as a result of blood flow (Dessalles et al., 2021). Application of shear stress promotes the actin cytoskeleton to remodel and results in bovine aEC elongation and alignment along the direction of flow (Osborn et al., 2006). In isolated bovine aECs, the application of flow promotes a synchronised initiation and elongation of actin filaments (Choi and Helmke, 2008). Whilst in the absence of flow, actin polymerisation is uncoordinated and non-directional (Choi and Helmke, 2008). Only a few studies have investigated the combined effects of substrate stiffness and shear stress. In bovine aECs, substrate stiffness was found to modulate the endothelial response to shear stress (Kohn et al., 2015). In these cells, increased substrate stiffness impeded shear stress induced alignment and junctional integrity of ECs (Kohn et al., 2015). An interplay between stiffness and shear stress has also been reported in human aECs. Under high levels of shear stress, increased substrate stiffness promoted an expansion of aEC area (Lai et al., 2023). However, under low levels of shear stress, increased substrate stiffness resulted in a reduction of cell area (Lai et al., 2023). Regions of low or disturbed shear stress are atherogenic, meaning much of the research on shear stress is focused on its involvement in atherosclerosis (Cunningham and Gotlieb, 2005). How shear stress changes during ageing is unclear, with conflicting studies showing that ageing can increase or decrease shear stress (Arenas et al., 2006; Lantz et al., 2015). Like substrate stiffness, endothelial response to shear stress is regulated by endothelial origin. Shear stress induces greater polarisation in aortic as opposed to veinous ECs, whilst brain mECs undergo no polarisation at all (Dessalles et al., 2021). Due to the size and undulating nature of the microvasculature, shear stress across the microvascular networks is highly variable (Hogan et al., 2019). How mECs respond to physiological shear stress and how microvascular shear stress changes during ageing are topics that requires further investigation.

Cell-ECM force transduction is mediated by FAs. In bovine aECs, substrate stiffness drives FA maturation, with more and larger FAs observed near the cell periphery (Lampi et al., 2017). In contrast, we found that LmECs and MmECs only develop mature FAs when cultured on glass substrates. Meanwhile, over a physiological range of substrate stiffnesses, nascent adhesions are observed at the tips of lamellipodia on 25 kPa substrates, with fibrillar adhesions on 72 kPa substrates. Endothelial FA maturation is generally hierarchical, with small α5β1-integrin-rich nascent adhesions forming first. As nascent adhesions mature, α5β1-integrin is substituted for αvβ3-integrin and additional proteins are recruited to form mature FA complexes (Rossier et al., 2012; Wolfenson et al., 2013). Fibrillar adhesions form during actomyosin-induced ECM remodelling, as α5β1-integrin-rich fibrils emerge from mature FAs and translocate towards the cell centre (Zamir et al., 2000). Fibrillar adhesion formation is regulated by both the rigidity and deformability of a substrate (Zamir et al., 2000). Although glass is more rigid, it is less deformable. It therefore takes longer for mECs cultured on glass to form fibrillar adhesions (Benwell et al., 2024).

Endothelial integrin-activation and expression is known to be regulated by substrate stiffness (Kretschmer et al., 2023; Sack et al., 2016). Integrin-based FA complexes function as multiprotein signalling hubs that regulate a diverse range of cellular processes in health and disease (Mishra and Manavathi, 2021). Our findings establish that mEC response to substrate stiffness is not ubiquitous. Instead, lung and mammary gland-derived mEC proliferation and migration are differentially regulated by changes in substrate stiffness, whilst stiffness-induced changes in mEC morphology are consistent between the two lines. Therefore, it is highly likely that minute differences in FA complex composition are responsible for differences between LmEC and MmEC response to substrate stiffness. As a next step, future research should aim to understand the molecular mechanism through which substrate stiffness induces differential responses in mECs depending on their organ of origin.

5. Conclusion

Matrix stiffness increases with age, and enhanced matrix stiffness drives endothelial dysfunction. Previous studies have shown that ECs are sensitive to changes in substrate stiffness. However, it was unknown whether the endothelial organ of origin regulated how microvascular

ECs respond to increased stiffness. We therefore isolated mECs from either the mouse lung or mammary gland and compared their response to age/disease-associated increases in substrate stiffness. We show that mEC response to substrate stiffness is programmed by their organ of origin (Fig. 6). We found that stiffness-induced changes in mEC proliferation and migration were dependent on mEC origin. However, some stiffness-induced changes, such as mEC morphology, were consistent between both mEC lines. Additionally, we show that increased substrate stiffness promotes an enlargement of mEC volume. This suggests that substrate stiffness may drive endothelial hypertrophy, a known precursor of numerous diseases. Our findings highlight the importance of considering endothelial origin in experimental design. HUVECs and bovine aECs are readily available, well-characterised EC lines. However, observations made in those cell lines, or one particular mEC line, cannot be fully translated to all ECs due to differences that arise based on endothelial origin. To conclude, we identify that endothelial origin regulates cellular response to changes in ECM stiffness. Further research is required to identify the molecular mechanisms and pathways through which enhanced ECM stiffness induces organ-specific endothelial dysfunction.

CRediT authorship contribution statement

Rana Haidari: Investigation, Formal analysis. **Wesley J. Fowler:** Methodology, Visualization. **Stephen D. Robinson:** Resources, Supervision, Funding acquisition, Writing – review & editing. **Robert T. Johnson:** Conceptualization, Investigation, Validation, Visualization, Formal analysis, Supervision, Funding acquisition, Writing – original draft. **Derek T. Warren:** Methodology, Supervision, Funding acquisition, Writing – review & editing.

Ethical statement

No live animals were used in this study. Mice used for endothelial cell line generation were bred in accordance with UK Home Office regulations and the European Legal Framework for the Protection of Animals used for Scientific Purposes (European Directive 86/609/EEC).

Data availability

Data supporting the findings of this study are available from the corresponding author upon request.

Funding

This work was funded by a Biotechnology and Biological Sciences Research Council Research Grant (BB/T007699/1) awarded to Derek T. Warren, a Big C appeal studentship bursary (Reference SB22-01) awarded to Rana Haidari, and a UKRI Biotechnology and Biological Sciences Research Council Norwich Research Park Doctoral Training Partnership PhD Studentship (BB/M011216/11) awarded to Wesley J. Fowler.

Declaration of competing interest

The authors declare that they have no known competing financial interests or personal relationships that could have appeared to influence the work reported in this paper.

Acknowledgements

The authors would like to acknowledge Dr. Tracey Swingler, firstly for her introduction of Rana Haidari to us, and secondly for her support and mentoring of countless PhD students and postdocs within the Biomedical Research Centre, University of East Anglia. Additionally, we gratefully acknowledge Brigita Medelyte, Jon Herskind, and Ida Bang Hansen of Aarhus University for their thorough review and valuable feedback on this manuscript.

Appendix A. Supplementary data

Supplementary data to this article can be found online at https://doi.org/10.1016/j.crphys.2025.100140.

Data availability

Data will be made available on request.

References

Acerbi, I., Cassereau, L., Dean, I., Shi, Q., Au, A., Park, C., Chen, Y.Y., Liphardt, J., Hwang, E.S., Weaver, V.M., 2015. Human breast cancer invasion and aggression correlates with ECM stiffening and immune cell infiltration. Integr. Biol. 7, 1120–1134. https://doi.org/10.1039/c5ib00040h.

Ahmed, S., Johnson, R.T., Solanki, R., Afewerki, T., Wostear, F., Warren, D.T., 2022. Using polyacrylamide hydrogels to model physiological aortic stiffness reveals that microtubules are critical regulators of isolated smooth muscle cell morphology and contractility. Front. Pharmacol. 13. https://doi.org/10.3389/fphar.2022.836710.

Alenghat, F.J., Ingber, D.E., 2002. Mechanotransduction: all signals point to cytoskeleton, matrix, and integrins. Sci. STKE 2002. https://doi.org/10.1126/stke.2002.119.pe6 pe6–pe6.

Alghamdi, A.A.A., Benwell, C.J., Atkinson, S.J., Lambert, J., Johnson, R.T., Robinson, S. D., 2020. NRP2 as an emerging angiogenic player; promoting endothelial cell adhesion and migration by regulating recycling of α5 integrin. Front. Cell Dev. Biol. 8. https://doi.org/10.3389/fcell.2020.00395.

Arani, A., Murphy, M.C., Glaser, K.J., Manduca, A., Lake, D.S., Kruse, S.A., Jack, C.R., Ehman, R.L., Huston, J., 2015. Measuring the effects of aging and sex on regional brain stiffness with MR elastography in healthy older adults. Neuroimage 111, 59–64. https://doi.org/10.1016/j.neuroimage.2015.02.016.

Arenas, I.A., Xu, Y., Davidge, S.T., 2006. Age-associated impairment in vasorelaxation to fluid shear stress in the female vasculature is improved by TNF-α antagonism. Am. J. Physiol. Heart Circ. Physiol. 290, H1259–H1263. https://doi.org/10.1152/ajpheart.00990.2005.

Atkinson, S.J., Gontarczyk, A.M., Alghamdi, A.A., Ellison, T.S., Johnson, R.T., Fowler, W. J., Kirkup, B.M., Silva, B.C., Harry, B.E., Schneider, J.G., Weilbaecher, K.N., Mogensen, M.M., Bass, M.D., Parsons, M., Edwards, D.R., Robinson, S.D., 2018. The β3-integrin endothelial adhesome regulates microtubule-dependent cell migration. EMBO Rep. 19, e44578. https://doi.org/10.15252/embr.201744578.

Balestrini, J.L., Chaudhry, S., Sarrazy, V., Koehler, A., Hinz, B., 2012. The mechanical memory of lung myofibroblasts. Integr. Biol. 4, 410–421. https://doi.org/10.1039/c2ib00149g.

Bastounis, E.E., Yeh, Y.-T., Theriot, J.A., 2019. Subendothelial stiffness alters endothelial cell traction force generation while exerting a minimal effect on the transcriptome. Sci. Rep. 9, 18209. https://doi.org/10.1038/s41598-019-54336-2.

Benwell, C.J., Johnson, R.T., Taylor, J.A.G.E., Lambert, J., Robinson, S.D., 2024. A proteomics approach to isolating neuropilin-dependent α5 integrin trafficking pathways: neuropilin 1 and 2 co-traffic α5 integrin through endosomal p120RasGAP to promote polarised fibronectin fibrillogenesis in endothelial cells. Commun. Biol. 7, 1–19. https://doi.org/10.1038/s42003-024-06320-4.

Benwell, C.J., Johnson, R.T., Taylor, J.A.G.E., Price, C.A., Robinson, S.D., 2022. Endothelial VEGFR coreceptors neuropilin-1 and neuropilin-2 are essential for tumor angiogenesis. Cancer Research Communications 2, 1626–1640. https://doi.org/10.1158/2767-9764.CRC-22-0250.

Boisen, L., Drasbek, K.R., Pedersen, A.S., Kristensen, P., 2010. Evaluation of endothelial cell culture as a model system of vascular ageing. Experimental Gerontology, Biomarkers of Ageing: from Molecular Biology to Clinical Perspectives 45, 779–787. https://doi.org/10.1016/j.exger.2010.06.003.

Bordeleau, F., Mason, B.N., Lollis, E.M., Mazzola, M., Zanotelli, M.R., Somasegar, S., Califano, J.P., Montague, C., LaValley, D.J., Huynh, J., Mencia-Trinchant, N., Negrón Abril, Y.L., Hassane, D.C., Bonassar, L.J., Butcher, J.T., Weiss, R.S., Reinhart-King, C. A., 2017. Matrix stiffening promotes a tumor vasculature phenotype. Proc. Natl. Acad. Sci. USA 114, 492–497. https://doi.org/10.1073/pnas.1613855114.

Burgess, J.K., Mauad, T., Tjin, G., Karlsson, J.C., Westergren-Thorsson, G., 2016. The extracellular matrix – the under-recognized element in lung disease? J. Pathol. 240, 397–409. https://doi.org/10.1002/path.4808.

Butcher, D.T., Alliston, T., Weaver, V.M., 2009. A tense situation: forcing tumour progression. Nat. Rev. Cancer 9, 108–122. https://doi.org/10.1038/nrc2544.

Byfield, F.J., Reen, R.K., Shentu, T.-P., Levitan, I., Gooch, K.J., 2009. Endothelial actin and cell stiffness is modulated by substrate stiffness in 2D and 3D. J. Biomech. 42, 1114–1119. https://doi.org/10.1016/j.jbiomech.2009.02.012.

Califano, J.P., Reinhart-King, C.A., 2010. Substrate stiffness and cell area predict cellular traction stresses in single cells and cells in contact. Cell. Mol. Bioeng. 3, 68–75. https://doi.org/10.1007/s12195-010-0102-6.

Canver, A.C., Ngo, O., Urbano, R.L., Clyne, A.M., 2016. Endothelial directed collective migration depends on substrate stiffness via localized myosin contractility and cell-matrix interactions. Journal of Biomechanics, SI: Motility and dynamics of living cells in health, disease and healing 49, 1369–1380. https://doi.org/10.1016/j.jbiomech.2015.12.037.

Chanda, A., Singh, G., 2023. Tissues in functional organs—low stiffness. In: Chanda, A., Singh, G. (Eds.), Mechanical Properties of Human Tissues. Springer Nature, Singapore, pp. 33–48. https://doi.org/10.1007/978-981-99-2225-3_4.

Choi, C.K., Helmke, B.P., 2008. Short-term shear stress induces rapid actin dynamics in living endothelial cells. Mol. Cell. BioMech. 5, 247–258. https://doi.org/10.3970/mcb.2008.005.247.

Connelly, P.J., Azizi, Z., Alipour, P., Delles, C., Pilote, L., Raparelli, V., 2021. The importance of gender to understand sex differences in cardiovascular disease. Can. J. Cardiol. 37, 699–710. https://doi.org/10.1016/j.cjca.2021.02.005.

Cox, T.R., Erler, J.T., 2011. Remodeling and homeostasis of the extracellular matrix: implications for fibrotic diseases and cancer. Disease Models & Mechanisms 4, 165–178. https://doi.org/10.1242/dmm.004077.

Cunningham, K.S., Gotlieb, A.I., 2005. The role of shear stress in the pathogenesis of atherosclerosis. Lab. Invest. 85, 9–23. https://doi.org/10.1038/labinvest.3700215.

Derricks, K.E., Trinkaus-Randall, V., Nugent, M.A., 2015. Extracellular matrix stiffness modulates VEGF calcium signaling in endothelial cells: individual cell and population analysis. Integr. Biol. 7, 1011–1025. https://doi.org/10.1039/c5ib00140d.

Dessalles, C.A., Leclech, C., Castagnino, A., Barakat, A.I., 2021. Integration of substrate- and flow-derived stresses in endothelial cell mechanobiology. Commun. Biol. 4, 1–15. https://doi.org/10.1038/s42003-021-02285-w.

Ding, Y., Floren, M., Tan, W., 2017. High-throughput screening of vascular endothelium-destructive or protective microenvironments: cooperative actions of extracellular matrix composition, stiffness, and structure. Adv. Healthcare Mater. 6, 1601426. https://doi.org/10.1002/adhm.201601426.

Eby, S.F., Cloud, B.A., Brandenburg, J.E., Giambini, H., Song, P., Chen, S., LeBrasseur, N. K., An, K.-N., 2015. Shear wave elastography of passive skeletal muscle stiffness: influences of sex and age throughout adulthood. Clin. BioMech. 30, 22–27. https://doi.org/10.1016/j.clinbiomech.2014.11.011.

Ellison, T.S., Atkinson, S.J., Steri, V., Kirkup, B.M., Preedy, M.E.J., Johnson, R.T., Ruhrberg, C., Edwards, D.R., Schneider, J.G., Weilbaecher, K., Robinson, S.D., 2015. Suppression of β3-integrin in mice triggers a neuropilin-1-dependent change in focal adhesion remodelling that can be targeted to block pathological angiogenesis. Disease Models & Mechanisms 8, 1105–1119. https://doi.org/10.1242/dmm.019927.

Fang, Y., Wu, D., Birukov, K.G., 2019. Mechanosensing and mechanoregulation of endothelial cell functions. Compr. Physiol. 9, 873–904. https://doi.org/10.1002/cphy.c180020.

Gao, Z., Chen, Z., Sun, A., Deng, X., 2019. Gender differences in cardiovascular disease. Medicine in Novel Technology and Devices 4, 100025. https://doi.org/10.1016/j.medntd.2019.100025.

Gauci, S., Cartledge, S., Redfern, J., Gallagher, R., Huxley, R., Lee, C.M.Y., Vassallo, A., O'Neil, A., 2022. Biology, bias, or both? The contribution of sex and gender to the disparity in cardiovascular outcomes between women and men. Curr. Atherosclerosis Rep. 24, 701–708. https://doi.org/10.1007/s11883-022-01046-2.

Gifre-Renom, L., Daems, M., Luttun, A., Jones, E.A.V., 2022. Organ-specific endothelial cell differentiation and impact of microenvironmental cues on endothelial heterogeneity. Int. J. Mol. Sci. 23, 1477. https://doi.org/10.3390/ijms23031477.

Gjorevski, N., Nelson, C.M., 2009. Bidirectional extracellular matrix signaling during tissue morphogenesis. Cytokine & growth factor reviews, bone morphogenetic proteins. Stem Cells and Regenerative Medicine 20, 459–465. https://doi.org/10.1016/j.cytogfr.2009.10.013.

Guimarães, C.F., Gasperini, L., Marques, A.P., Reis, R.L., 2020. The stiffness of living tissues and its implications for tissue engineering. Nat. Rev. Mater. 5, 351–370. https://doi.org/10.1038/s41578-019-0169-1.

Guo, J., Huang, X., Dou, L., Yan, M., Shen, T., Tang, W., Li, J., 2022. Aging and aging-related diseases: from molecular mechanisms to interventions and treatments. Signal Transduct. Targeted Ther. 7, 1–40. https://doi.org/10.1038/s41392-022-01251-0.

Guo, T., He, C., Venado, A., Zhou, Y., 2022. Extracellular matrix stiffness in lung health and disease. Compr. Physiol. 12, 3523–3558. https://doi.org/10.1002/cphy.c210032.

Hartman, R.J.G., Kapteijn, D.M.C., Haitjema, S., Bekker, M.N., Mokry, M., Pasterkamp, G., Civelek, M., den Ruijter, H.M., 2020. Intrinsic transcriptomic sex differences in human endothelial cells at birth and in adults are associated with coronary artery disease targets. Sci. Rep. 10, 12367. https://doi.org/10.1038/s41598-020-69451-8.

Hofman, P., van Blijswijk, B.C., Gaillard, P.J., Vrensen, G.F.J.M., Schlingemann, R.O., 2001. Endothelial cell hypertrophy induced by vascular endothelial growth factor in the retina: new insights into the pathogenesis of capillary nonperfusion. Arch. Ophthalmol. 119, 861–866. https://doi.org/10.1001/archopht.119.6.861.

Hogan, B., Shen, Z., Zhang, H., Misbah, C., Barakat, A.I., 2019. Shear stress in the microvasculature: influence of red blood cell morphology and endothelial wall undulation. Biomech. Model. Mechanobiol. 18, 1095–1109. https://doi.org/10.1007/s10237-019-01130-8.

Hooglugt, A., Klatt, O., Huveneers, S., 2022. Vascular stiffening and endothelial dysfunction in atherosclerosis. Curr. Opin. Lipidol. 33, 353. https://doi.org/10.1097/MOL.0000000000000852.

Hsu, T., Nguyen-Tran, H.-H., Trojanowska, M., 2019. Active roles of dysfunctional vascular endothelium in fibrosis and cancer. J. Biomed. Sci. 26, 86. https://doi.org/10.1186/s12929-019-0580-3.

Huang, C., Liu, L., You, Z., Zhao, Y., Dong, J., Du, Y., Ogawa, R., 2017. Endothelial dysfunction and mechanobiology in pathological cutaneous scarring: lessons learned from soft tissue fibrosis. Br. J. Dermatol. 177, 1248–1255. https://doi.org/10.1111/bjd.15576.

Huveneers, S., Daemen, M.J.A.P., Hordijk, P.L., 2015. Between rho(k) and a hard place. Circ. Res. 116, 895–908. https://doi.org/10.1161/CIRCRESAHA.116.305720.

Jacques, D., Bkaily, G., 2019. Endocardial endothelial cell hypertrophy takes place during the development of hereditary cardiomyopathy. Mol. Cell. Biochem. 453, 157–161. https://doi.org/10.1007/s11010-018-3440-7.

Johnson, R.T., Solanki, R., Warren, D.T., 2021. Mechanical programming of arterial smooth muscle cells in health and ageing. Biophys Rev 13, 757–768. https://doi.org/10.1007/s12551-021-00833-6.

Johnson, R.T., Solanki, R., Wostear, F., Ahmed, S., Taylor, J.C.K., Rees, J., Abel, G., McColl, J., Jørgensen, H.F., Morris, C.J., Bidula, S., Warren, D.T., 2024a. Piezo1-mediated regulation of smooth muscle cell volume in response to enhanced extracellular matrix rigidity. Br. J. Pharmacol. 181, 1576–1595. https://doi.org/10.1111/bph.16294.

Johnson, R.T., Wostear, F., Solanki, R., Steward, O., Bradford, A., Morris, C., Bidula, S., Warren, D.T., 2024b. A microtubule stability switch alters isolated vascular smooth muscle calcium flux in response to matrix rigidity. Journal of Cell Science jcs 262310. https://doi.org/10.1242/jcs.262310.

Juin, A., Planus, E., Guillemot, F., Horakova, P., Albiges-Rizo, C., Génot, E., Rosenbaum, J., Moreau, V., Saltel, F., 2013. Extracellular matrix rigidity controls podosome induction in microvascular endothelial cells. Biol. Cell. 105, 46–57. https://doi.org/10.1111/boc.201200037.

Kalucka, J., Rooij, L.P.M.H. de, Goveia, J., Rohlenova, K., Dumas, S.J., Meta, E., Conchinha, N.V., Taverna, F., Teuwen, L.-A., Veys, K., García-Caballero, M., Khan, S., Geldhof, V., Sokol, L., Chen, R., Treps, L., Borri, M., Zeeuw, P. de, Dubois, C., Karakach, T.K., Falkenberg, K.D., Parys, M., Yin, X., Vinckier, S., Du, Y., Fenton, R.A., Schoonjans, L., Dewerchin, M., Eelen, G., Thienpont, B., Lin, L., Bolund, L., Li, X., Luo, Y., Carmeliet, P., 2020. Single-cell transcriptome atlas of murine endothelial cells. Cell 180, 764–779.e20. https://doi.org/10.1016/j.cell.2020.01.015.

Kohn, J.C., Zhou, D.W., Bordeleau, F., Zhou, A.L., Mason, B.N., Mitchell, M.J., King, M. R., Reinhart-King, C.A., 2015. Cooperative effects of matrix stiffness and fluid shear stress on endothelial cell behavior. Biophys. J. 108, 471–478. https://doi.org/10.1016/j.bpj.2014.12.023.

Kretschmer, M., Mamistvalov, R., Sprinzak, D., Vollmar, A.M., Zahler, S., 2023. Matrix stiffness regulates Notch signaling activity in endothelial cells. J. Cell Sci. 136, jcs260442. https://doi.org/10.1242/jcs.260442.

Kwon, S., Yang, W., Moon, D., Kim, K.S., 2020. Comparison of cancer cell elasticity by cell type. J. Cancer 11, 5403–5412. https://doi.org/10.7150/jca.45897.

Lai, A., Zhou, Y., Thurgood, P., Chheang, C., Chandra Sekar, N., Nguyen, N., Peter, K., Khoshmanesh, K., Baratchi, S., 2023. Endothelial response to the combined biomechanics of vessel stiffness and shear stress is regulated via Piezo1. ACS Appl. Mater. Interfaces 15, 59103–59116. https://doi.org/10.1021/acsami.3c07756.

Lampi, M.C., Guvendiren, M., Burdick, J.A., Reinhart-King, C.A., 2017. Photopatterned hydrogels to investigate the endothelial cell response to matrix stiffness heterogeneity. ACS Biomater. Sci. Eng. 3, 3007–3016. https://doi.org/10.1021/acsbiomaterials.6b00633.

Lantz, J., Renner, J., Länne, T., Karlsson, M., 2015. Is aortic wall shear stress affected by aging? An image-based numerical study with two age groups. Med. Eng. Phys. 37, 265–271. https://doi.org/10.1016/j.medengphy.2014.12.011.

LaValley, D.J., Zanotelli, M.R., Bordeleau, F., Wang, W., Schwager, S.C., Reinhart-King, C.A., 2017. Matrix stiffness enhances VEGFR-2 internalization, signaling, and proliferation in endothelial cells. Converg. Sci. Phys. Oncol 3, 044001. https://doi.org/10.1088/2057-1739/aa9263.

Lee, S., Kumar, S., 2016. Actomyosin stress fiber mechanosensing in 2D and 3D. F1000Res 5. https://doi.org/10.12688/f1000research.8800.1. F1000 Faculty Rev-2261.

Lu, P., Takai, K., Weaver, V.M., Werb, Z., 2011. Extracellular matrix degradation and remodeling in development and disease. Cold Spring Harbor Perspect. Biol. 3, a005058. https://doi.org/10.1101/cshperspect.a005058.

Luque, T., Melo, E., Garreta, E., Cortiella, J., Nichols, J., Farré, R., Navajas, D., 2013. Local micromechanical properties of decellularized lung scaffolds measured with atomic force microscopy. Acta Biomater. 9, 6852–6859. https://doi.org/10.1016/j.actbio.2013.02.044.

Mammoto, A., Mammoto, T., Kanapathipillai, M., Wing Yung, C., Jiang, E., Jiang, A., Lofgren, K., Gee, E.P.S., Ingber, D.E., 2013. Control of lung vascular permeability and endotoxin-induced pulmonary oedema by changes in extracellular matrix mechanics. Nat. Commun. 4, 1759. https://doi.org/10.1038/ncomms2774.

Mason, B.N., Starchenko, A., Williams, R.M., Bonassar, L.J., Reinhart-King, C.A., 2013. Tuning three-dimensional collagen matrix stiffness independently of collagen concentration modulates endothelial cell behavior. Acta Biomater. 9, 4635–4644. https://doi.org/10.1016/j.actbio.2012.08.007.

McKee, C.T., Last, J.A., Russell, P., Murphy, C.J., 2011. Indentation versus tensile measurements of Young's modulus for soft biological tissues. Tissue Eng., Part B 17, 155–164. https://doi.org/10.1089/ten.teb.2010.0520.

Melo, E., Cárdenes, N., Garreta, E., Luque, T., Rojas, M., Navajas, D., Farré, R., 2014. Inhomogeneity of local stiffness in the extracellular matrix scaffold of fibrotic mouse lungs. J. Mech. Behav. Biomed. Mater. 37, 186–195. https://doi.org/10.1016/j.jmbbm.2014.05.019.

Merz, A.A., Cheng, S., 2016. Sex differences in cardiovascular ageing. Heart 102, 825–831. https://doi.org/10.1136/heartjnl-2015-308769.

Miller, A.E., Hu, P., Barker, T.H., 2020. Feeling things out: bidirectional signaling of the cell–ECM interface, implications in the mechanobiology of cell spreading, migration, proliferation, and differentiation. Adv. Healthcare Mater. 9, 1901445. https://doi.org/10.1002/adhm.201901445.

Minaisah, R.-M., Cox, S., Warren, D.T., 2016. The use of polyacrylamide hydrogels to study the effects of matrix stiffness on nuclear envelope properties. In: Shackleton, S., Collas, P., Schirmer, E.C. (Eds.), The Nuclear Envelope: Methods and

Protocols. Springer, New York, NY, pp. 233–239. https://doi.org/10.1007/978-1-4939-3530-7_15.
Mishra, Y.G., Manavathi, B., 2021. Focal adhesion dynamics in cellular function and disease. Cell. Signal. 85, 110046. https://doi.org/10.1016/j.cellsig.2021.110046.
Moccia, C., Cherubini, M., Fortea, M., Akinbote, A., Padmanaban, P., Beltran-Sastre, V., Haase, K., 2023. Mammary microvessels are sensitive to menstrual cycle sex hormones. Adv. Sci. 10, 2302561. https://doi.org/10.1002/advs.202302561.
Moeller, J., Denisin, A.K., Sim, J.Y., Wilson, R.E., Ribeiro, A.J.S., Pruitt, B.L., 2018. Controlling cell shape on hydrogels using lift-off protein patterning. PLoS One 13, e0189901. https://doi.org/10.1371/journal.pone.0189901.
Mohindra, R., Agrawal, D.K., Thankam, F.G., 2021. Altered vascular extracellular matrix in the pathogenesis of atherosclerosis. J. of Cardiovasc. Trans. Res. 14, 647–660. https://doi.org/10.1007/s12265-020-10091-8.
Navindaran, K., Kang, J.S., Moon, K., 2023. Techniques for characterizing mechanical properties of soft tissues. J. Mech. Behav. Biomed. Mater. 138, 105575. https://doi.org/10.1016/j.jmbbm.2022.105575.
Ni, C.-W., Kumar, S., Ankeny, C.J., Jo, H., 2014. Development of immortalized mouse aortic endothelial cell lines. Vasc. Cell 6, 7. https://doi.org/10.1186/2045-824X-6-7.
Niccoli, T., Partridge, L., 2012. Ageing as a risk factor for disease. Curr. Biol. 22, R741–R752. https://doi.org/10.1016/j.cub.2012.07.024.
Ohashi, K., Fujiwara, S., Mizuno, K., 2017. Roles of the cytoskeleton, cell adhesion and rho signalling in mechanosensing and mechanotransduction. J. Biochem. 161, 245–254. https://doi.org/10.1093/jb/mvw082.
Osborn, E.A., Rabodzey, A., Dewey, C.F., Hartwig, J.H., 2006. Endothelial actin cytoskeleton remodeling during mechanostimulation with fluid shear stress. Am. J. Physiol. Cell Physiol. 290, C444–C452. https://doi.org/10.1152/ajpcell.00218.2005.
Paszek, M.J., Zahir, N., Johnson, K.R., Lakins, J.N., Rozenberg, G.I., Gefen, A., Reinhart-King, C.A., Margulies, S.S., Dembo, M., Boettiger, D., Hammer, D.A., Weaver, V.M., 2005. Tensional homeostasis and the malignant phenotype. Cancer Cell 8, 241–254. https://doi.org/10.1016/j.ccr.2005.08.010.
Porter, L., Minaisah, R.-M., Ahmed, S., Ali, S., Norton, R., Zhang, Q., Ferraro, E., Molenaar, C., Holt, M., Cox, S., Fountain, S., Shanahan, C., Warren, D., 2020. SUN1/2 are essential for RhoA/ROCK-regulated actomyosin activity in isolated vascular smooth muscle cells. Cells 9, 132. https://doi.org/10.3390/cells9010132.
Pospelov, A.D., Kutova, O.M., Efremov, Y.M., Nekrasova, A.A., Trushina, D.B., Gefter, S. D., Cherkasova, E.I., Timofeeva, L.B., Timashev, P.S., Zvyagin, A.V., Balalaeva, I.V., 2023. Breast cancer cell type and biomechanical properties of decellularized mouse organs drives tumor cell colonization. Cells 12, 2030. https://doi.org/10.3390/cells12162030.
Prasain, N., Stevens, T., 2009. The actin cytoskeleton in endothelial cell phenotypes. Microvascular Research, Concepts in Microvascular Endothelial Barrier Regulation in Health and Disease 77, 53–63. https://doi.org/10.1016/j.mvr.2008.09.012.
Ramião, N.G., Martins, P.S., Rynkevic, R., Fernandes, A.A., Barroso, M., Santos, D.C., 2016. Biomechanical properties of breast tissue, a state-of-the-art review. Biomech. Model. Mechanobiol. 15, 1307–1323. https://doi.org/10.1007/s10237-016-0763-8.
Reynolds, L.E., Hodivala-Dilke, K.M., 2006. Primary mouse endothelial cell culture for assays of angiogenesis. In: Brooks, S.A., Harris, A. (Eds.), Breast Cancer Research Protocols. Humana Press, Totowa, NJ, pp. 503–509. https://doi.org/10.1385/1-59259-969-9, 503.
Ricard, N., Bailly, S., Guignabert, C., Simons, M., 2021. The quiescent endothelium: signalling pathways regulating organ-specific endothelial normalcy. Nat. Rev. Cardiol. 18, 565–580. https://doi.org/10.1038/s41569-021-00517-4.
Rossier, O., Octeau, V., Sibarita, J.-B., Leduc, C., Tessier, B., Nair, D., Gatterdam, V., Destaing, O., Albigès-Rizo, C., Tampé, R., Cognet, L., Choquet, D., Lounis, B., Giannone, G., 2012. Integrins β1 and β3 exhibit distinct dynamic nanoscale organizations inside focal adhesions. Nat. Cell Biol. 14, 1057–1067. https://doi.org/10.1038/ncb2588.
Sack, K.D., Teran, M., Nugent, M.A., 2016. Extracellular matrix stiffness controls VEGF signaling and processing in endothelial cells. J. Cell. Physiol. 231, 2026–2039. https://doi.org/10.1002/jcp.25312.
Schedin, P., Keely, P.J., 2011. Mammary gland ECM remodeling, stiffness, and mechanosignaling in normal development and tumor progression. Cold Spring Harbor Perspect. Biol. 3, a003228. https://doi.org/10.1101/cshperspect.a003228.
Schindelin, J., Arganda-Carreras, I., Frise, E., Kaynig, V., Longair, M., Pietzsch, T., Preibisch, S., Rueden, C., Saalfeld, S., Schmid, B., Tinevez, J.-Y., White, D.J., Hartenstein, V., Eliceiri, K., Tomancak, P., Cardona, A., 2012. Fiji: an open-source platform for biological-image analysis. Nat. Methods 9, 676–682. https://doi.org/10.1038/nmeth.2019.
Schmauck-Medina, T., Molière, A., Lautrup, S., Zhang, J., Chlopicki, S., Madsen, H.B., Cao, S., Soendenbroe, C., Mansell, E., Vestergaard, M.B., Li, Z., Shiloh, Y., Opresko, P.L., Egly, J.-M., Kirkwood, T., Verdin, E., Bohr, V.A., Cox, L.S., Stevnsner, T., Rasmussen, L.J., Fang, E.F., 2022. New hallmarks of ageing: a 2022 Copenhagen ageing meeting summary. Aging (Albany NY) 14, 6829–6839. https://doi.org/10.18632/aging.204248.
Schnellmann, R., Ntekoumes, D., Choudhury, M.I., Sun, S., Wei, Z., Gerecht, S., 2022. Stiffening matrix induces age-mediated microvascular phenotype through increased cell contractility and destabilization of adherens junctions. Adv. Sci. 9, 2201483. https://doi.org/10.1002/advs.202201483.
Schnittler, H., Taha, M., Schnittler, M.O., Taha, A.A., Lindemann, N., Seebach, J., 2014. Actin filament dynamics and endothelial cell junctions: the Ying and Yang between stabilization and motion. Cell Tissue Res. 355, 529–543. https://doi.org/10.1007/s00441-014-1856-2.
Shen, J., Xie, Y., Liu, Z., Zhang, S., Wang, Yaping, Jia, L., Wang, Yidong, Cai, Z., Ma, H., Xiang, M., 2018. Increased myocardial stiffness activates cardiac microvascular endothelial cell via VEGF paracrine signaling in cardiac hypertrophy. J. Mol. Cell. Cardiol. 122, 140–151. https://doi.org/10.1016/j.yjmcc.2018.08.014.
Southern, B.D., Grove, L.M., Rahaman, S.O., Abraham, S., Scheraga, R.G., Niese, K.A., Sun, H., Herzog, E.L., Liu, F., Tschumperlin, D.J., Egelhoff, T.T., Rosenfeld, S.S., Olman, M.A., 2016. Matrix-driven myosin II mediates the pro-fibrotic fibroblast phenotype. J. Biol. Chem. 291, 6083–6095. https://doi.org/10.1074/jbc.M115.712380.
Statzer, C., Park, J.Y.C., Ewald, C.Y., 2023. Extracellular matrix dynamics as an emerging yet understudied hallmark of aging and longevity. Aging Dis 14, 670–693. https://doi.org/10.14336/AD.2022.1116.
Stroka, K.M., Aranda-Espinoza, H., 2011. Effects of morphology vs. Cell–cell interactions on endothelial cell stiffness. Cell. Mol. Bioeng. 4, 9–27. https://doi.org/10.1007/s12195-010-0142-y.
Sugimoto, H., Hamano, Y., Charytan, D., Cosgrove, D., Kieran, M., Sudhakar, A., Kalluri, R., 2003. Neutralization of circulating vascular endothelial growth factor (VEGF) by anti-VEGF antibodies and soluble VEGF receptor 1 (sFlt-1) induces proteinuria. J. Biol. Chem. 278, 12605–12608. https://doi.org/10.1074/jbc.C300012200.
Tavora, B., Reynolds, L.E., Batista, S., Demircioglu, F., Fernandez, I., Lechertier, T., Lees, D.M., Wong, P.-P., Alexopoulou, A., Elia, G., Clear, A., Ledoux, A., Hunter, J., Perkins, N., Gribben, J.G., Hodivala-Dilke, K.M., 2014. Endothelial-cell FAK targeting sensitizes tumours to DNA-damaging therapy. Nature 514, 112–116. https://doi.org/10.1038/nature13541.
Theocharis, A.D., Manou, D., Karamanos, N.K., 2019. The extracellular matrix as a multitasking player in disease. FEBS J. 286, 2830–2869. https://doi.org/10.1111/febs.14818.
Wolfenson, H., Lavelin, I., Geiger, B., 2013. Dynamic regulation of the structure and functions of integrin adhesions. Dev. Cell 24, 447–458. https://doi.org/10.1016/j.devcel.2013.02.012.
Wood, J.A., Shah, N.M., McKee, C.T., Hughbanks, M.L., Liliensiek, S.J., Russell, P., Murphy, C.J., 2011. The role of substratum compliance of hydrogels on vascular endothelial cell behavior. Biomaterials 32, 5056–5064. https://doi.org/10.1016/j.biomaterials.2011.03.054.
Wu, D., Birukov, K., 2019. Endothelial cell mechano-metabolomic coupling to disease states in the lung microvasculature. Front. Bioeng. Biotechnol. 7, 172. https://doi.org/10.3389/fbioe.2019.00172.
Xu, Z., Chen, Y., Wang, Y., Han, W., Xu, W., Liao, X., Zhang, T., Wang, G., 2023. Matrix stiffness, endothelial dysfunction and atherosclerosis. Mol. Biol. Rep. 50, 7027–7041. https://doi.org/10.1007/s11033-023-08502-5.
Yeh, Y.-T., Hur, S.S., Chang, J., Wang, K.-C., Chiu, J.-J., Li, Y.-S., Chien, S., 2012. Matrix stiffness regulates endothelial cell proliferation through septin 9. PLoS One 7, e46889. https://doi.org/10.1371/journal.pone.0046889.
Zamir, E., Katz, M., Posen, Y., Erez, N., Yamada, K.M., Katz, B.-Z., Lin, S., Lin, D.C., Bershadsky, A., Kam, Z., Geiger, B., 2000. Dynamics and segregation of cell–matrix adhesions in cultured fibroblasts. Nat. Cell Biol. 2, 191–196. https://doi.org/10.1038/35008607.
Zhong, J., Yang, Y., Liao, L., Zhang, C., 2020. Matrix stiffness-regulated cellular functions under different dimensionalities. Biomater. Sci. 8, 2734–2755. https://doi.org/10.1039/C9BM01809C.
Zuchi, C., Tritto, I., Carluccio, E., Mattei, C., Cattadori, G., Ambrosio, G., 2020. Role of endothelial dysfunction in heart failure. Heart Fail. Rev. 25, 21–30. https://doi.org/10.1007/s10741-019-09881-3.